95601

LA-UR- 98-1861

Approved for public release; distribution is unlimited.

Title: Generation and compression of a Target Plasma for Magnetized Target Fusion

Author(s): Ronald C. Kirkpatrick, NIS-9
Irvin R. Lindemuth, Anthony G. Sgro, X-PA
Peter T. Sheehey, X-NH
Joyce A. Guzik, X-TA
Ronald W. Moses, T-3
Richard Siemon, STB-FE
Frederick J. Wysocki, Don A. Baker, Richard A. Gerwin, Kurt F. Schoenberg, P-24

Submitted to: DOE OFFICE OF SCIENTIFIC AND TECHNICAL INFORMATION (OSTI)

Los Alamos
NATIONAL LABORATORY

DISCLAIMER

Generation and compression of a Target Plasma for Magnetized Target Fusion

Ronald C. Kirkpatrick*, Irvin R. Lindemuth, Peter T. Sheehey, Joyce A. Guzik, Frederick J. Wysocki, Don A. Baker, Ronald W. Moses, Anthony G. Sgro, Richard Siemon, Richard A. Gerwin, and Kurt F. Schoenberg
Los Alamos National Laboratory

Francis Y.C. Thio
Massey University, NZ

Abstract

This is the final report of a three-year, Laboratory Directed Research and Development (LDRD) project at the Los Alamos National Laboratory (LANL). Magnetized target fusion (MTF) is intermediate between the two very different approaches to fusion: inertial and magnetic confinement fusion (ICF and MCF). Results from collaboration with a Russian MTF team on their MAGO experiments suggest they have a target plasma suitable for compression to provide an MTF proof of principle. This LDRD project had two main objectives: First, to provide a computational basis for experimental investigation of an alternative MTF plasma, and second to explore the physics and computational needs for a continuing program. Secondary objectives included analytic and computational support for MTF experiments. The first objective was fulfilled. The second main objective has several facets to be described in the body of this report. Finally, we have developed tools for analyzing data collected on the MAGO and LDRD experiments, and have tested them on limited MAGO data.

Background and Research Objectives

Here we briefly summarize our previous reports and papers on magnetized target fusion (MTF) and magnetic compression (MAGO).

Theoretical Basis for MTF

MTF is intermediate between two very different mainline approaches to fusion: inertial confinement fusion (ICF) and magnetic confinement fusion (MCF). It is based on the fact that a magnetic field suppresses electron thermal conduction in a sufficiently hot plasma. Electron thermal conduction is the major energy loss mechanism for the wall confined, unmagnetized plasmas produced in most designs for fusion ignition targets for ICF [1]. However, for ICF simply imposing a magnetic field on existing ignition target designs does little to suppress electron thermal conduction. This is because the density is so high that the mean collision time in the plasma is short, leading to a small magnetization

*Principal Investigator, e-mail: rck@lanl.gov

parameter, the cyclotron frequency- collision time product (ωt). In the absence of conduction loss, bremsstrahlung would become the dominant ICF energy loss mechanism. Therefore, MTF must operate in a lower density regime than ICF, so that both conduction and radiation losses are reduced. For similar fusion plasma mass, this leads to a larger target containing a gaseous deuterium and tritium (DT) fusion fuel at about 0.01 to 1 mg/cc.

The required level of magnetic field for insulation of the fusion fuel from loss to the surrounding wall is sufficiently low that synchrotron radiation and magnetic field energy are only small perturbations on the fusion fuel dynamics. If initially the plasma has a high ratio of internal energy to magnetic energy β, then it will always be so as the plasma is compressed in all three dimensions. With sufficiently reduced energy loss rates the plasma can be compressed relatively adiabatically to fusion temperatures by squeezing it with the confining vessel [2,3]. With the reduced energy loss rates, the rate of compression as determined by the implosion velocity and geometry of the confining vessel can be much lower than needed for ICF. In ICF the confining vessel is a spherical shell that is symmetrically and rapidly imploded to a very small final radius. One embodiment of MTF would be similar, except the implosion velocity would be over an order of magnitude lower.

Fusion ignition is not required for all fusion energy schemes, but ignition is what makes ICF a viable fusion energy concept. Fusion ignition relies on "self-heating", which means that the fusion energy release in the form of energetic reaction products (neutrons alpha particles for DT fusion) is at least partially deposited in the fusion plasma as these particles pass through it. For ICF the critical parameter that determines whether the fusion self-heating overbalances the energy losses from the fusion plasma is the areal density ρR. It must exceed approximately 0.3 gm/cm^2 for fusion ignition to occur. For this very low value of areal density, the neutrons deposit very little energy, so the DT alpha particles are the major source of self-heating. The efficiency of the burn that follows also depends on an areal density, but that of the imploding part of the target (fusion fuel plus imploded confining vessel), and therefore, the gain depends on the ρR as well. For DT alpha transport in MTF an additional parameter is important. The ρR is augmented by a field times radius parameter BR.

Because the energetic charged particles in a magnetized plasma are turned in the field, their path in the fusion fuel is lengthened. In a hot plasma the magnetic field is essentially frozen in place relative to the plasma, so that the compression of the plasma by the imploded confining vessel also compresses the field, which can reach many megagauss. The critical parameter is the gyroradius. If it is much smaller than the fusion plasma radius, then a significant part of the energy of charged fusion products will be

deposited to self-heat the plasma. The critical value corresponds to a field times radius product (BR) of 0.3 MG-cm, but the higher the better. The very low ρR typical of MTF is significantly augmented by the high BR, so that fusion ignition can occur for MTF. In one study a particle tracking code was used to calculate the fraction of DT alpha particle energy deposited in spherical volume of homogeneous magnetized plasma with a pure azimuthal field [4]. Some results for that study are shown in Figure 1. Figure 2 shows the dependence of the fractional deposition on temperature for a ρR of 0.001 gm/cm^2.

Previous MTF Experiments

Previous MTF research included the Sandia National Laboratory "Phi-target" experiments [5, 6], the only series of experiments documented in available scientific literature in which a plasma known to be magnetized was compressed. This target resembled the Greek character Φ (see Figure 3). Despite the very interesting results from that series of experiments, the research was not pursued, and other embodiments of the MTF concept such as the Fast Liner [2] were unable to attract the support needed for a firm proof of principle. A mapping of the parameter space for MTF [7] showed the significant features of this approach, which have steadily attracted more attention. Since the All-Russia Scientific Institute for Experimental Physics (VNIIEF) revealed their on-going interest in this approach to thermonuclear fusion, Los Alamos National Laboratory (LANL) and VNIIEF have done joint, target-plasma-generation experiments relevant to MTF referred to as MAGO (transliteration of the Russian acronym for magnetic compression) [8]. The MAGO II experiment appears to have achieved on the order of 200 eV and over 100 KG (which will be discussed below), so that adiabatic compression with a relatively small convergence could bring the plasma to fusion temperatures.

Potential Impact of MTF

MTF potentially represents a significant advance in fusion technology. Because MTF targets are larger and can be imploded slower, the power and intensity for driving the target to fusion ignition are potentially orders of magnitude lower. However, for the same mass of fusion fuel the energy required for ignition is about the same, simply because the same thermal energy must be supplied to the fusion fuel to raise it to the ignition temperature [3]. Ignition of a given design of fusion target requires that the fusion driver (laser, particle beam, or otherwise) simultaneously supply sufficient energy, power, and intensity. For example, at this time lasers are sufficiently powerful and intense to drive appropriate designs of ICF targets to ignition, but are not sufficiently energetic. The anticipated National Ignition Facility (NIF) at Livermore, California, is intended to provide all three, that is, sufficient energy, power, and intensity on target. The attractiveness of MTF is that the reduced power and intensity requirements needed for MTF targets admit

pulsed-power machines as potential drivers for fusion targets. Direct pulsed power has never been a contender as an ICF driver, because of an inability to supply the necessary power and intensity on target. However, pulsed power machines can easily supply sufficient energy, power, and intensity for MTF and are more efficient overall than laser or other beam drivers. For higher efficiency drivers, lower gain targets become attractive for fusion power.

MTF provides a development path for fusion energy that is mid-way between the two dominant approaches to fusion energy. We desire a scientific proof of principle which demonstrates that compression of a magnetized plasma heats it in accord with MTF theory. Previous MTF studies [3,7] have emphasized that existing pulsed power technology is adequate for a scientific proof of principle, and probably sufficient for experimental exploration beyond. This would allow an economical and significant advance of fusion science and technology. The reasons for this assertion were summarized above.

It should be noted that MTF is a concept that may have many diverse embodiments, some purely for experimental investigation of MTF, and potentially others for applications such as fusion power production and space propulsion. We have taken the position that the most important first task for research on any fusion concept is to provide a proof of principle. Once that is done, the concept becomes a candidate for consideration as a possible approach to fusion energy production or some other application. In addition, there may be many unanticipated applications of fusion besides electric power generation.

Project Objective

This LDRD project had two main objectives: First, to provide a computational basis for experimental investigation of a Z-pinch approach to generation of an MTF plasma, and second, to explore the physics and computational needs for a continuing program. Secondary objectives included analytic and computational support for MTF experiments. In the section on scientific approach and accomplishments we present the progress that has been made over the past three years in creating a target plasma that is suitable for compression in a future scientific proof-of-principle experiment for MTF. We also present here some forward looking work we have done on MTF theory.

Importance to LANL's Science and Technology Base and National R&D Needs

The importance to both the Los Alamos Science and Technology Base (STB) and national research and development needs is substantial. Los Alamos has had a historical commitment to fusion technology and now has a need to find a way to study fusion physics without weapons testing. MTF may provide a more benign setting for studying fusion

physics and provide experimental data useful for benchmarking our computer codes in the coming years. Despite previous fusion work, MTF is a relatively unexplored approach to fusion, and a lot of research is needed to realize its potential. We will discuss these aspects in the paragraphs below.

Historical Commitment, Continuing Need, and Promise

Thermonuclear fusion, in one form or another, has been a major part of the Los Alamos National Laboratory's mission almost from its inception. In 1945 Rolf Landshoff enunciated one of the underlying principles of MTF; that is, the reduction of electron thermal conductivity in a plasma by a strong magnetic field, and Enrico Fermi suggested its application to realizing fusion. However, this little known suggestion was never pursued in its original form, but instead the idea of creating a magnetic bottle superseded it. In addition to the important role of thermonuclear (TN) fusion in the nuclear weapons program, if it can be successfully controlled TN fusion offers one of the few long-term hopes to meet the massive future world energy requirements that have been predicted. As the Laboratory redefines its activities in a post-Cold War environment, new initiatives in controlled fusion can exercise nearly all the theoretical, computational, and experimental skills necessary for preservation of nuclear weapons design and testing capabilities in a scientifically exciting and challenging endeavor, can provide science-based stockpile stewardship with potentially important sources of fusion neutrons and plasma at thermonuclear temperature, and can make contributions to the nation's quest for a nearly inexhaustible source of energy.

MTF Leadership

Although one basic principle of MTF dates back to 1945, MTF is a relatively unexplored approach to fusion which has been recognized as a legitimate, separate concept only in the last few years. In many ways MTF can be considered a marriage between the traditional magnetic and inertial confinement approaches, and can potentially eliminate some of the pitfalls of the other two. In particular, MTF requires simpler, smaller, and considerably less expensive systems than either magnetic confinement or inertial confinement (e.g., "laser" or heavy ion) fusion. The instabilities that plague traditional approaches to fusion are potentially mitigated in MTF due to wall confinement, shockless acceleration and relatively low velocity (e.g. ~ 1 cm/μsec) of the pusher, and low required convergence ratios (e.g., 10:1).

Los Alamos has been a center for US theoretical work on MTF. Growing worldwide interest in MTF can be attributed to LANL's leadership and the recognition that the two mainline approaches to controlled fusion have reached crucial turning points in their development paths: each now requires capital investments of $1-10 billion for ignition-scale

facilities (NIF, ITER). Facing budget realities and Congressional pressure, the Department of Energy Office of Fusion Energy Science (OFES) is restructuring to increase its emphasis on plasma science and low-cost alternative concepts, of which MTF is a prime candidate.

Collaboration

Additional significant stimulants to the emerging international interest in MTF are experiments Los Alamos has jointly performed with its Russian counterpart, the All-Russian Scientific Research Institute of Experimental Physics (VNIIEF) at Sarov (Arzamas-16). VNIIEF, motivated by Sakharov's initial ideas, and as a basic sciences initiative within the Russian nuclear weapons complex, appears to have devoted substantial efforts to develop technology related to MTF. Hence, VNIIEF has made advances in pulsed power technology, plasma formation techniques and implosion systems. A series of four joint experiments have investigated a VNIIEF-invented plasma formation scheme, known here by the Russian acronym for MTF, MAGO. In addition, in an August 1996 joint experiment, a VNIIEF Disk Explosive Magnetic Generator (DEMG) delivered a 100-MA electrical current pulse to an imploding aluminum liner, which achieved an implosion kinetic energy of more than 20 MJ. These conditions are certainly adequate for an MTF implosion driver.

Although not performed in an MTF context, recent Phillips Laboratory experiments have injected an unmagnetized plasma into a quasi-spherical magnetically driven liner and have demonstrated that the liner can seal the plasma injection ports and compress the plasma. Recent LANL liner implosion experiments, again not performed in an MTF context, have begun to delineate the physics issues of high-performance magnetically driven liners. Los Alamos is also developing a Z-pinch target plasma under other LDRD funding.

With existing DEMGs appearing to provide adequate energy, and with a variety of existing or near-term nonexplosive pulsed power facilities (e.g., Colt, Pegasus, and Atlas at Los Alamos; Saturn and PBFA-Z at Sandia; and SHIVA-STAR at Phillips) capable of plasma formation and/or liner implosion experiments with modest modifications, it appears that the physics issues of MTF can be explored without a major facility investment. This possibility has clearly been recognized by the international scientific community. Furthermore, VNIIEF was awarded two grants from the International Science and Technology Center for further experimentation and development of the VNIIEF approach to MTF.

Missing from the international community at the present time are diagnostic techniques that can clearly confirm that a target plasma is suitable for subsequent implosion, and diagnostics that can determine plasma behavior under implosion conditions.

Because plasma parameters in MTF are substantially different (e.g., orders of magnitude in plasma density) from those in traditional controlled fusion and nuclear weapons, substantial work is required to adapt some of the extensive diagnostic techniques developed in these programs for use in MTF. Old techniques need to be improved and new techniques may need to be developed.

Similarly missing from the international community is the capability to do integrated computational design and modeling of liner-on-plasma implosion systems. While LANL has achieved substantial success in modeling the MAGO experiments with an AGEX magnetohydrodynamic (MHD) code, and in modeling imploding liners with other codes, it does not appear likely than any "off-the-shelf" capability can satisfactorily model a combined liner-plasma system. In fact the few candidate codes have, for the most part, not even been adequately benchmarked in the plasma formation regime. This represents important future work.

We have begun a collaboration with one of the French CEA Labs to jointly acquire and share data on the Colt-bank target-plasma-generation experiment that will be described below. In addition, we hosted a professor from New Zealand in FY 1997 who is now initiating an MTF research effort there.

Project Contributions

The computational tools developed in this project can now be used to analyze data in future experiments and to improve computational techniques in mainline production codes. The validation of the mainline production codes in the high-energy-density regimes of MTF will enhance their growing use in a Science-Based Stockpile Stewardship (SBSS) context. The potential for MTF contributions to SBSS extend beyond the necessary and very important role of providing a focal point for large-scale computer code validation in laboratory regimes not likely to be accessed by any other means. A number of SBSS applications have been suggested for the hot plasma and intense thermonuclear neutron sources that may result from liner-on-plasma systems designed with the capability developed in this project. These include: (1) possible neutralization of nuclear, biological, and chemical (NBC)terrorist devices; (2) nuclear emergency response (NEST) activities; (3) intense neutron source for nuclear criticality studies; and (4) resolving nuclear weapons computer codes and physics model uncertainties. More work will be required to validate these suggested applications.

A useful SBSS role for MTF should justify increased DOE Defense Programs funding; and this project has helped to place LANL in a favorable position for funding from the newly restructured DOE Office of Fusion Energy Sciences (OFES). Hence, this project represents an investment in the future of the fusion-related community at Los Alamos.

Long-Term Prospects

Unlike many shorter-term stockpile stewardship activities that exercise only a subset of the skills needed for maintaining nuclear weapons expertise, the quest for fusion without fission represents a "scientific grand challenge" that will ultimately stretch the skills of weapons design teams and hopefully lead to "beating our swords into plowshares". Because MTF has no weapons potential, it is unclassified and publishable, and the research that it enables should attract and retain highly qualified scientists, and involve more university and foreign collaborators. Of course, any direct stockpile stewardship applications will remain classified, but because of the potential of fusion in an energy (and possibly other) context, MTF should serve as an example of using some former weapons design skills for peaceful purposes while retaining the weapons design skills that may be needed in the future.

The Lab now has the opportunity to capitalize on our MTF progress.

Scientific Approach and Accomplishments

The major accomplishments of this project were the computational definition of an alternate target-plasma-generation approach, the development of an automated method for analyzing the filtered silicon diode data from the MTF target plasma experiments, and the analysis of the MAGO II data to obtain temperature and density histories for that target plasma. There were several secondary accomplishments. One was calculation of the DT-fusion alpha-particle -energy deposition and its dependence on areal density and magnetization of the fusion plasma, as well as concurrent development of an efficient approach to computing the DT alpha transport in a dynamic MTF plasma. Another was the study of the plasma-wall interaction problem. In addition this project has attracted the attention and support of a growing number of fusion scientists. As awareness of MTF grows in the wider fusion community at universities and other DOE labs, the prospects for DOE funding of this activity increase significantly. We will discuss below each of these in the above order.

Target Plasma Development

A few years ago when the Laboratory still had the High Density Zeta Pinch (HDZP), Marx bank pulsed-power machine, LDRD supported experiments were performed in which a discharge through cryogenic deuterium fibers created a strong pinch and produced a neutron producing plasma. The intention was to create a very fast Z-pinch that would "out run" the well-known plasma instabilities by attaining a stabilizing condition inside the plasma before the instabilities could develop. If this state could be reached, the Bennett relation would predict that some fusion gain could be achieved. This

proved to not be possible with the HDZP machine, nor has any other research group demonstrated stabilization of the pinch. Peter Sheehey was able to take the results from calculations with the MHD code MHRDR written by Irv Lindemuth and reconstruct shadowgrams and interferograms for comparison with the data. He provided the correct interpretation of the data: the instabilities that developed had not been observable with the early diagnostics, but better diagnostics were consistent with instabilities that grew rapidly and ultimately disrupted the pinch enough to prevent continued compression of the central plasma. We now have considerable confidence in this code because of its success in explaining not only the data for the HDZP experiment, but also that of the MAGO experiments and other complex plasma experiments done over the past decade.

The HDZP direct Z-pinch approach to fusion was not successful, but it did demonstrate a technology that could create a hot, magnetized plasma, and the computations used to understand it showed that as the instabilities developed, a hot, unstable, magnetized plasma consistent with the data was created. In the configuration used in the HDZP experiments the plasma continued to expand and soon cooled and dispersed. Since some of the Sandia Phi-targets had involved a discharge through CD_2 fibers that became the target plasma compressed by the exploding pusher in those experiments, it was natural to investigate the possibility of a similar target plasma creation approach for our new MTF initiative. Peter Sheehey performed MHRDR calculations for a configuration that used a metal cylinder as the return path for the current discharged through a cryogenic deuterium fiber. The volume was closed by an insulator at one end of the "can" and a metal "lid" on the other end. This is shown in Figure 4. The circuit used for the calculation modeled the Colt capacitor bank and produced a relatively slow rising current as compared with the HDZP machine.

MHRDR calculations of the configuration of a cryogenic deuterium fiber in a "can" showed that instabilities did develop early on, but rather than disrupting the pinch they allowed the magnetic field to diffuse into the plasma as it expanded. Because the wall limited the expansion of the plasma, it ultimately evolved into a 1-D configuration and made periodic adjustments toward what appeared to be a Kadomsev stable profile. The Kadomsev-like temperature, density, and magnetic field profiles include a wide range of values, but the combined average values exceed what our MTF survey codes say are the minimum for an MTF target plasma. After the current peaks and then declines, the average temperature of the plasma remains near the peak value. Since the plasma is confined, the average density cannot change, and the code predicts that the plasma electrically isolates itself so that the current that magnetizes it continues to flow within the plasma. Some of the results are shown in Figure 5.

Target Plasma Generation Experiment

On the basis of the above calculations, an LDRD- supported experimental effort was mounted that was intended to demonstrate the properties of the wall-supported Z-pinch and to demonstrate plasma conditions meeting the minimum requirements for a MTF initial target plasma. This experimental effort is being fielded on the Colt capacitor bank, one module of the previous configuration of the Pegasus pulsed-power machine. The configuration chosen for these experiments is shown in Figure 6. To date no cryogenic fibers have been fielded. The fiber-making technology involves a good deal of art as well as science, and some of the former expertise was lost with retirements, etc.

Uniform gas-fill plasma-generation experiments are underway using the Colt facility. It is a 0.25 MJ, 2-3 μs rise-time capacitor bank. The goal of these experiments is to produce a diffuse Z-pinch inside a 2-cm radius by 2-cm high conducting cylindrical metal container using a static gas fill of hydrogen or deuterium gas in the range of 0.5 to 2 torr. Thus far the diagnostics include an array of 12 B-dot probes, a framing camera, a gated OMA visible spectrometer, a time-resolved monochrometer, filtered silicon photodiodes, neutron yield, and plasma-density interferometers. These diagnostics show that a plasma is produced in the containment region that lasts roughly 10 to 20 μs with a maximum plasma density exceeding 10^{18} cm^{-3}. Some data is shown in Figure 7. The capabilities discussed in the next section will be used to analyze this data in the near future. Also, as soon as the fiber maker is operational, cryogenic fiber shots will begin.

Diagnostic Development

One diagnostic that has proved to be relatively robust, and therefore valuable, on two of the MAGO experiments is the filtered silicon diode. We intend to use this diagnostic to acquire data on the wall-supported Z-pinch experiments on the Colt bank. In fact, some data is already available, but not yet analyzed. Development of this diagnostic on the MAGO experiments should prove invaluable for analyzing the continuing Colt bank experiments. In order to understand the data from this diagnostic it has been necessary to develop a system of codes to analyze it. This is on several levels. First, it is possible, given a sufficient number of filtered diode signals, to reconstruct a crude spectrum for the emission from a plasma. However, the first MAGO data resulted from a diagnostic development effort on the MAGO II experiment done at Los Alamos, and only a limited number of diodes were fielded. Only three of these could be used together to diagnose the plasma along the same path through the plasma. This meant that spectral reconstruction was not possible. By making use of the MHRDR MHD code (mentioned above), which was used to calculate the plasma formation process for the MAGO experiments, we could get the run of temperature and density along the path where these three diodes looked, but

another code was required to calculate the details of the emission, because 0.01 % neon was added to the DT gas in the MAGO II chambers. The neon was intended to provide lines observable with x-ray spectroscopy, but the spectrogram was fogged by activation before it could be retrieved after the experiment.

Analysis Code

The Los Alamos ZAP code was chosen to help in analysis of the filtered silicon diode data. It is a one-dimensional (1-D) code written by Gordon Olson that handles the detailed atomic physics necessary for treating hot plasmas that are far from thermodynamic equilibrium (non-LTE) and has been used in the past for a variety of non-LTE radiation transport problems. It requires atomic models, which consist of all the relevant transition probabilities, photoionization cross sections, collisional excitation and ionization cross sections (or the velocity averaged collision strengths), etc. ZAP can also be used to predict emission from other plasmas and future experiments. In addition this code can provide spectral profiles for individual lines, so its potential is great for various future experiments. However, ZAP was intended for a different use that made direct use for analyzing the MAGO data difficult, so we modified it to provide a version that we could use with the MHRDR code results and provide a simulated diode signal history.

We were disappointed in the initial results with ZAP, but eventually discovered a bug in the modified version of the code whenever a string of multiple calculations were attempted for a temporal history. The unmodified code gave reliable results. In the interim, we developed an alternative approach to analyzing the data, a description of which we will present here, to be followed by some improvements using results from multiple runs of the unmodified ZAP code.

For MAGO II there were a total of 5 lines of sight defined by five diagnostic access holes drilled through the walls into chamber #2 (see Figure 8). Four of these looked along lines parallel to the axis of the experiment at a radius of 6 cm. A single silicon diode provided a signal for each 6-cm line of sight. Three of these four had filters and one had none. In addition there was a blind silicon diode intended to measure the effect of neutrons and gammas that gave no signal, suggesting that there should be no such contribution to the filtered diode signals. Figure 9 shows the mounting of a filtered diode in an assembly for mounting on the chamber wall. The access hole and placement of the diodes for MAGO II defined a solid angle of 0.0026 steradians and the diodes were 0.05 mm^2 in area. Figure 10 shows the filtered diode response curves. Typical silicon photodiode diode characteristic curves are shown in Figure 11, and the detector circuit is shown in Figure 12. There are many details regarding calibration and fielding [9] not discussed here.

The unfiltered diode was clearly overdriven and produced data that was not readily interpretable, but the three filtered diodes gave clean signals out to about 5 μs after the signal began to rise in the most sensitive of the filtered diodes. Shortly after that all three signals abruptly rose to much higher levels than their previous peak values. A detailed study was made of possible shocks generated by the sudden creation of a magnetized plasma in chamber #2 that might travel up the diagnostic access hole and destroy the filters [10], but we only mention it here.

Data Analysis

The data for the three MAGO II filtered silicon diodes looking along the 6-cm line of sight are shown in Figure 13. Before the first discharge occurs in the MAGO chambers the signals are very low with a noise level indicated by small positive and negative excursions about the mean, and this is used in later analysis of the data. In Figure 13, zero on the time axis corresponds to 347.0 μs in the MAGO III data files. For MAGO II 0.01 % neon impurity was added to the 10 torr of DT that filled both chambers. This was done to insure that at least some lines would appear in the spectrum that might help in temperature and density determination when the x-ray spectra were analyzed after the shot. Inclusion of the neon made it necessary to use ZAP to assess the importance of the lines for the filtered silicon diode analysis.

The data from MAGO II is very limited; there are only three useable detector signals for the 6-cm radius lines of sight. This means that only two independent ratios are available to infer information on the characteristic spectrum of the plasma emission. The third independent piece of data (signal level) provides the intensity of the plasma emission. Therefore, if we wish to learn something about the plasma, we are forced to make some assumptions and proceed to test these assumptions.

An initial analysis of the MAGO II data was presented at the Megagauss VII (MG7) conference held in Sarov, Russia, in August of 1996. It used 5 types of idealized spectra: hydrogen bremsstrahlung ($I_\nu \sim g_{ff}(n)\exp[-h\nu/kT_e]$), Planck ($I_\nu \sim \nu^3/[\exp(h\nu/kT_e) -1]$), flat with a cutoff energy ($I_\nu = 1$ for $h\nu < E_c$, 0 otherwise), a square profile at a specific energy, and an exponential ($I_\nu \sim \exp(-h\nu/kT_e)$). The procedure involved multiplying the spectra for various characteristic temperatures (or photon energies) times the filtered diode response functions and integrating with respect to energy to get expected diode responses for each temperature or energy. Then, the theoretical diode response ratios at each time were compared with the data to find the best fit for each spectral type for each time in the data.

This allowed us to get a characteristic electron temperature history (or photon energy of the dominant spectral feature) for the MAGO plasma in chamber #2 for each of the five spectral types. The inferred history for each type is shown in Figure 14. Implicit

in this analysis is that the result for each time in the history represents a characteristic or spatially averaged value. Nothing can be said about the spatial temperature distribution, so that for simplicity, the plasma can be assumed to be uniform.

During the time when the signal-to-noise ratio (S/N) is high, the bremsstrahlung spectrum generally gives the best rms fit to the data, but other spectral types sometimes are better (see Figure 15). However, it should be noted that when the S/N is low, the results for all types are wildly varying, even though for the times of low S/N the fits are better. This is partly because the noise level was taken into account in making the comparison. The early measure of the noise mentioned above was added to the theoretical and measured responses, so that as the signals drop, a realistic result is obtained. That is, as the signal becomes comparable to the noise, almost all (noisy) theoretical response ratios compare equally well with the (noisy) data.

The regularity during time of high S/N is to be emphasized for all spectral types. As expected, the inferred Planck temperatures are significantly lower than the brems-strahlung and exponential temperatures, the latter two being rather close, but also reflecting the fact that there is a difference in their spectral character. After the peak emission the apparent decay in temperature slows to a characteristic decay time of about 10 μs. If the spectrum were from an optically thick plasma at the temperature history of the Planck curve in Figure 14, then the radiation would overwhelm the detectors, so this must not be the case. If the detectors were responding to a single strong line, then the spectral position of that line would have to be time varying, so it wouldn't fit the description of a single strong line. Of course, two or more strong lines acting in concert could be responsible for the history of the detector signals. Then one would have to inquire about the source of such lines acting in concert. One reasonable explanation would be that there are changing ionization stages for some impurity species for which the dominant lines for each have different centers of gravity in frequency space.

Assuming that the bremsstrahlung spectrum is the best choice of the five spectral types for a DT plasma with 0.01% neon impurity, it is possible to get an estimated density history for a given temperature history by noting that the emission should scale as the square of the plasma density. As shown in Figure 16, the density rises to nearly 10^{19}/cc during the peak emission, but then falls to about 10^{18}/cc at late time.

At about 7.6 μs the signal for the most sensitive filtered diode rises abruptly and appears to saturate. Shortly thereafter the other two diode signals also rise abruptly. While the analysis gives temperatures and densities for the microsecond that follows, we are reluctant to accept these values as meaningful, because we judge the data to be flawed.

Elsewhere, we have presented a detailed study of the possible shocks generated by the sudden pressure rise in chamber #2 and subsequently travel up the diagnostic holes [10].

ZAP Results

Because the MAGO II experiment used 0.01% Ne as a tracer in the DT gas, significant emission was expected from Ne VIII at a photon energy of about 1 Kev. In order to take the effect of these lines into account we synthesized spectra for a variety of isobaric temperature and density profiles with the ZAP code (discussed above) and obtained the filter responses for these synthesized spectra. Then we repeated the process described in the previous paragraphs, but rather than having five spectral types, we used the synthesized spectra with the 0.01% neon included. This provided the MAGO II temperature history shown in Figure 17. The commensurate estimated density history derived for these spectra is shown in Figure 18. The points (x's and o's for 1-T and 2-T) are the simple averages of the temperatures and densities computed using MHRDR for a path through the 2-D mesh that corresponds to the diagnostic line of sight.

We concluded that the MAGO II data is consistent with emission from a ~200 eV, ~10^{18}/cc target plasma suitable for compression to provide a scientific proof of principle for magnetized target fusion. Also, the difference between the estimated density and the computed average density histories is consistent with an equivalent impurity of no more than 0.05% neon equivalent. A carefully chosen subset of the flawed MAGO III data roughly agrees with the MAGO II data. The data from these two experiments is too limited to rule out all other possible explanations, but it does rule the two mentioned above.

There appears to be good agreement with the results of the 2-D MHD code MHRDR, as analyzed using the ZAP non-LTE transport code, which suggests that we may now have predictive tools and an ability to analyze the data for fielding future experiments.

DT Alpha Transport

While fusion ignition (i.e., "self-heating") is not essential for all fusion energy concepts, it is of central importance for some such as ICF. Our survey code results showed that fusion gain is possible without ignition for MTF. Potentially, ignition would lead to higher gain. The main mechanism whereby the energy released in fusion reactions is returned to the plasma is by collisions between the energetic fusion products and the electrons and ions in the magnetized plasma. The two fusion reaction products for the most reactive fusion fuel, deuterium and tritium (DT), are a neutron and a helium nucleus. The latter is referred to as an alpha particle when very energetic, such as is the case when it is one of the products of a nuclear reaction (fission or fusion). The neutron is not expected to interact significantly within the fusion plasma, because it is electrically neutral. As the DT alpha undergoes coulomb collisions with the plasma constituents, it gives up its energy and

slows down. When the plasma is below about 10 KeV in temperature, the slowing occurs mainly by collisions with electrons, but above 10 KeV the ions become progressively more important. A complete treatment requires the inclusion of slowing by both. In addition, in a magnetized plasma the magnetic field turns the DT alpha. There is no force parallel to the magnetic field, but across it the force is proportional to the component of the velocity across the field times the field (**v x B**). Previous work concentrated on unmagnetized ICF plasmas [11-17] and tenuous magnetically confined plasmas [18-20]. In these limits several different assumptions are valid, but in the MTF context these assumptions break down. Also, the combined computational efficiency and accuracy required for use in dynamic MTF calculations is very high.

Particle Tracking Results

We have applied a particle tracking code to the case of a spherical volume of DT with homogeneous conditions [4] characterized by temperature, density, and an annular magnetic field flux density (ρ, T, B). Some results were already shown in Figures 1 and 2. The code used to get these results can be applied to much more complicated geometries and plasma distributions, but the computational expense increases rapidly as the magnetization parameter BR increases. Therefore, we sought a more efficient computational approach.

Crossing Time

We have developed some analytic relations that should ease the task of computing the DT alpha transport in the magnetized MTF plasma, and have developed an approach that uses these relations as well as transformations that greatly reduce the amount of numerical integration required. To avoid complicating the mathematics, here we illustrate the approach by making the assumption that the DT alpha particles do not interact with the plasma ions. In such a case in a plasma above 1 KeV, the velocity decreases exponentially with time:

$$v(t) = v_o\, e^{-t/\tau} \quad ,$$

where v_o is the initial velocity and t is the relaxation time due to Rutherford scattering with electrons. In an (x,y,z) coordinate system with the magnetic field B in the z direction and the x direction in the direction of **v x B**,

$$v_x(t) = v\, e^{-t/\tau} \cos(\omega t),$$

$$v_y(t) = v\, e^{-t/\tau} \sin(\omega t), \quad \text{and}$$

$$v_z(t) = v\, e^{-t/\tau},$$

so the path of a DT alpha particle ($\mathbf{s} = \int \mathbf{v}\, dt$) entering a homogeneous region at the origin will be:

$$x(t) = v_{yo}\tau \left(\omega\tau - e^{-t/\tau} (\sin \omega t + \omega\tau \cos \omega t) \right) / (1+\omega^2\tau^2)$$

$$y(t) = v_{yo}\tau \left(1 - e^{-t/\tau} (\cos \omega t - \omega\tau \sin \omega t) \right) / (1+ \omega^2\tau^2)$$

$$z(t) = v_{zo}\tau\,(\,1 - e^{-t/\tau}\,)\,.$$

The equation for a plane in that coordinate system is $A\,x + B\,y + C\,z = D$, where $A = d_x/d$, $B = d_y/d$, $C = d_z/d$, and $D = d$. Here, d is the distance between the point of entry into a computational cell at (0,0,0) and the plane defining one side of the cell.

Defining the coefficients

$$C_1 = (v_{yo}\tau\,(Awt + B) + C\,v_{zo}\tau - D\,)$$

$$C_2 = v_{yo}\tau\,A\,/\,C_1\,(1+\omega^2\tau^2)$$

$$C_3 = v_{yo}\tau\,B\,/\,C_1\,(1+\omega^2\tau^2),$$

$$C_4 = C\,v_{zo}\tau\,/\,C_1\ ,$$

and solving

$$e^{-t/\tau}\,[\,(C_2 - C_3\,\omega t)\sin\omega t\ +\ (C_3 + C_2\,\omega t)\cos\omega t\ + C_4] \ =\ 1$$

for the minimum crossing time t (there are potentially several crossings), and substituting into the above equations provides the exit point (x,y,z). Since there are more than one plane that define the cell, the minimum time among all of them must be found.

Tables can be made for the solutions to

$$e^{+wt/\omega\tau} = a\sin\omega t\ +\ b\cos\omega t + c\ ,$$

and an interpolation used to efficiently find solutions. The most convenient approach is to write the equation as $e^{q\theta} = a\sin\theta + b\cos\theta + c\ = R\sin(\theta + \phi) + c$, and then solve for $q(\theta) = 1/\omega\tau$, interpolating to get the θ that satisfies the equation for a given q. It should be noted that since $\omega\tau > 0$, $q > 0$ for physically meaningful solutions. For a given value of q there are multiple values of $\theta = \omega\tau$. Since we want the first crossing time, we choose the smallest value. For a zone defined by multiple planes ($A_n x + B_n y + C_n z = D_n$), the smallest from among all ωt_n is selected. This procedure can be extended to the case of slowing by ions and electrons, but becomes more complicated simply because the path for a DT alpha can't be expressed analytically for that case. The prospects for an efficient and sufficiently accurate DT charged-particle transport method for MTF should now be considered good.

Plasma/Wall Interaction

Some 1-D and 2-D magnetohydrodynamic (MHD) calculations of compression of a target plasma are underway. One major concern, the plasma wall interaction problem, is being investigated both analytically and computationally. The major concern is the introduction of impurities into the fusion plasma that could increase radiative losses from the plasma. While the ZAP code mentioned earlier can provide reliable calculations of enhanced radiation once the impurity level is known, we need to establish some measure of what impurity levels to expect. The Phi-target and MAGO experimental results might suggest that the level of impurities introduced is tolerable, since the calculations that have

had no impurities agree with the experimental data. However, it is possible that the target plasma formation phase is not as sensitive to impurities as the compression phase that follows. This aspect mainly depends on atomic number (Z) of the impurity.

The most difficult problem is associated with possible entrainment of wall material by a hydrogenic plasma flow along a wall consisting of a high-Z material. Such a flow might occur due to convective overturn that could develop due to the buoyancy of regions in the plasma where the magnetic pressure reduces the mass density. The physical problem is very difficult to handle directly in our present codes, and seems to demand the use of some phenomenological model for evolution of wall material into the plasma. Once the model is made available in a code (perhaps MHRDR), marker particles could be used to trace the migration of impurities.

There are other possible problems associated with the plasma/wall interaction. One is that the cooling of the plasma adjacent to the wall leaves that part of the plasma at lower β, so that the magnetic pressure of that part becomes more important in the compression of the magnetized plasma. Also, because the regions of higher magnetic field in an inwardly accelerated plasma have a mass deficiency, buoyancy forces come into play that can create convection that enhances cooling. Also, the magnetic field has a tendency to diffuse into the wall, which generates ohmic heating of the wall and reduces the strength of the field in the magnetized plasma. We have some computer codes that include this physics, so the greatest modeling (and experimental) uncertainty is potentially the impurity problem mentioned in the previous paragraph.

MTF System Model

As noted elsewhere in this report, a number of computer models have been developed to study MTF, including several 1-D and 2-D versions. Much of the aforementioned work is focused on issues of plasma compression, transport, and turbulence. This part of the project sought to assess the more global system performance while drawing on the results of existing models for the detailed descriptions of individual components. A so-called "0-D" computer model was written in *Mathematica* to represent the plasma, a compressible metal liner, the compression field, the capacitor bank, and the leads to the liner. The ODE solver of *Mathematica* is used to compute the following physical parameters as functions of time: liner current, inner and outer liner radii, bank energy, inductive energy, kinetic energy of liner, compression energy of liner, plasma energy, energy loss by thermal conduction, energy loss by radiation, ohmic losses in bank and leads, action integral ($\int J^2 dt$), plasma temperature, plasma density, B field at plasma edge, and fusion yield. Naturally, the most difficult features to model here are the thermal, radiation, and current transport in the plasma and liner. Many sources in the literature were

used to generate several analytic models of plasma transport ranging from the base case of adiabatic compression with no radiation, through classical 1-D thermal conduction plus bremsstrahlung, to turbulent thermal conduction plus bremsstrahlung, and then finally Bohm losses plus bremsstrahlung. The results of these calculations are presented in overlay plots to enable an assessment of which physics issues provide the greatest challenges to the MTF concept.

With the construction of the Atlas pulsed power facility at LANL, there is considerable interest in what Atlas could contribute to MTF research. Consequently, the "0-D" *Mathematica* code was used to investigate MTF with Atlas relevant parameters [9]. The following are typical parameters used in this study: bank energy = 36 MJ, transfer inductance = 10 nH, safety resistance = 2 mΩ, liner material = aluminum (largest burst condition), initial liner radius = 10 cm, liner cross sectional area = 5 cm^2, liner length = 10 cm, initial plasma density = $5x10^{17}$ cm^{-3}, initial plasma temperature = 200 eV, and initial edge magnetic field = 10 T.

Representative examples of this "0-D" model are shown in Figures 19-22. The results of these computations indicate several significant things to consider for MTF research. First, a 36 MJ bank appears to be sufficient to get Q > 1 (fusion energy > liner energy) for an ideal, adiabatically compressed plasma. Second, if sufficient plasma density and temperature can be achieved at the outset, a substantial level of thermal losses can be tolerated and still have the plasma reach fusion temperatures. Third, when the classical thermal and radiation losses to the liner are considered, the energy delivered to the liner will surely melt it, but vaporization only takes place late in the discharge. Fourth, the convergence ratios seen up through the Bohm scaling are on the order of 15-20. Optimization of liner mass and configuration should be able to bring this down to a ratio of 10, which is generally regarded as realistic. Finally, a large nonclassical energy transport to the liner poses a high probability that the liner will be vaporized before full compression is achieved. These calculations indicate that there is a possibility of getting Q > 1 with a machine on the scale of Atlas even considering classical transport, but "non classical" transport effects could cause significant reductions in anticipated performance.

A New Perspective

The "0-D" system model described above reflects the viewpoint of the majority of the fusion community. It is a different approach to analyzing MTF than that provided in the section entitled *Theoretical Basis* at the beginning of this report. We welcome this fresh viewpoint, and the recent involvement of several researchers from the controlled fusion community. They bring a lot of relevant experience and are better able to communicate the principles of MTF to the fusion community at large.

Conclusions

This magnetized target fusion LDRD project and a few other projects related to it have stimulated significant interest in the US and international fusion communities. Los Alamos is now well positioned as a leader in this new fusion field. A related joint theoretical/experimental LDRD project ("Magnetized Target Fusion: Experiments and Modeling") will continue in FY 1998 aimed at development of an MTF target plasma, design of liner-on-plasma implosions, and evaluation of science-based stockpile stewardship applications of MTF. This and related programmatic work should continue to prepare LANL to execute a liner-on-plasma MTF proof-of-principle experimental program.

Publications

1. Lindemuth, I.R., et al., "Target Plasma Formation for Magnetic Compression / Magnetized Target Fusion," Phys. Rev. Lett. 75, 1953 (1995).

2. Sheehey, P.T., and Lindemuth, I.R., "Hall and Two-Temperature Magnetohydrodynamic Simulation of Deuterium-Fiber-Initiated Z-Pinches," Physics of Plasmas 4, 146 (1997).

3. Sheehey, P.T., et al., "Computational and Experimental Investigation of Magnetized Target Fusion," Fusion Technology 30, 1355 (1996).

4. Kirkpatrick, R.C., "Energetic Alpha Particle Transport Method EATM" (Fifth Joint Conference on Computational Mathematics, Albuquerque, NM, September 2-5, 1997).

5. Kirkpatrick, R.C., "Magnetized Target Fusion (MTF): Relaxing the Driver Requirements," Second Symposium on Current Trends in International Fusion Research (Washington, DC, March 1997).

6. Kirkpatrick, R.C., "Report on Innovative Confinement Concepts Workshop," Second Symposium on Current Trends in International Fusion Research (Washington, DC, March 1997).

7. Kirkpatrick, R.C., "Transport Method for Energetic DT Alpha Particles in a Magnetized Plasma," (Innovative Confinement Concepts Workshop, Los Angeles, CA, March 3-8, 1997).

8. Kirkpatrick, R.C., "VNIIEF Magnetic Bubble Approach to an X*f*Ray Source," (International Pulsed Power Conference, Baltimore, MD, June 1997).

9. Kirkpatrick, R.C., and G. Idzorek, "Analysis of Filtered Silicon Diode Data from MAGO/MTF Experiments," (International Conference on Plasma Science, San Diego, CA, May 1997).

10. Kirkpatrick, R.C., and G. Idzorek, "Analysis of the Filtered Silicon Diode Data from the MAGO_II and MAGO_III Experiments," (Innovative Confinement Concepts Workshop, Los Angeles, CA, March 3-8, 1997).

11. Sheehey P.T., et al., "Computational Modeling of Wall-Supported Dense Z-Pinches," (Innovative Confinement Concepts Workshop, Los Angeles, CA, March 3-8, 1997).

12. Sheehey, P.T., et al., "Computational Modeling of Joint US-Russian Experiments Relevant to Magnetic Compression/Magnetized Target Fusion," (Fifth Joint Conference on Computational Mathematics, Albuquerque, NM, September 2-5, 1997).

13. Sheehey, P.T., et al., "Computational Modeling of Wall-Supported Dense Z-Pinches," (Dense Z-Pinch Conference, Vancouver, Canada, June 1997).

14. Wysocki, F.J., et al., "Progress with Developing a Target for Magnetized Target Fusion," (International Pulsed Power Conference, Baltimore, MD, June 6-8, 1997).

15. Kirkpatrick, R. C., Lindemuth, I. R. and Ward, M. S., "An Overview of Magnetized Target Fusion," Fusion Technology 27, p. 201 (1995).

16. Lindemuth, I.R., "Magnetized Target Fusion: Principles, Status, and International Collaboration," invited paper at 12th Heavy Ion Symposium, (Heidelberg, Germany, September 1997).

17. Lindemuth, I.R., et al., "US/Russian Collaboration in High-Energy-Density Physics Using High Explosive Pulsed Power," IEEE Transactions on Plasma Science (in press, 1997).

18. Lindemuth, I.R., et al., "The Los Alamos / Arzamas-16 Collaboration in High-Energy-Density Physics Using High Explosive Pulsed Power," plenary paper (International Pulsed Power Conference, Baltimore, MD, June 6-8, 1997).

19. Lindemuth, I.R., "MAGO/MTF: Controlled thermonuclear Fusion with Existing Pulsed Power Systems ???," (International Pulsed Power Conference, Baltimore, MD, June 6-8, 1997).

20. Lindemuth, I.R., "The Role of Z-pinches and Related Configurations in Magnetized Target Fusion (MTF)," to be published in the Proceedings of the 4th International Conference on Dense Z*f*Pinch Conference (Vancouver, Canada, June 1997).

21. Lindemuth, I.R., et al., "Magnetized Target Fusion (MTF): A Marrriage of of Inertial and Magnetic Confinement," invited paper at DOE Office of Fusion Energy Sciences Innovative Confinement Concepts Workshop (Los Angeles, CA, March 3-8, 1997) and Spring Workshop on Basic Science Applications of Pulsed Power (Monterey, CA, April 1997).

22. Kirkpatrick, R.C., and Lindemuth, I.R., "Magnetized Target Fusion, An Ultrahigh Energy Approach to an Unexplored Parameter Space," Current Trends in International Fusion Research, ed. E. Panarella, Plenum Press, New York, 1997.

23. Lindemuth, I.R., and Kirkpatrick, R.C., "Magnetized Target Fusion, An overview of the Concept", Current Trends in International Fusion Research, ed. E. Panarella, Plenum Press, New York, 1997.

24. Lindemuth, I.R., et al., "Magnetic Comnpression / Magnetized Target Fusion: A Marrriage of of Inertial and Magnetic Confinement," to be published in Proceedings of 16th IAEA International Conference on Plasma Physics and Controlled Fusion Research (Montreal, Canada, October 1996).

25. Lindemuth, I.R., et al., "The Plasma Formation Stage in Magnetic Comnpression / Magnetized Target Fusion (MAGO/MTF)," to be published in Proceedings of Seventh International Conference on Megagauss Magnetic Fields and Related Topics (Sarov, Russia, August 1996).

26. Lindemuth, I.R., Reinovsky, R.E., Younger, S.M., et al., "The Los Alamos / Arzamas-16 Collaboration in Ultrahigh Magnetic Fields and Ultrahigh Energy Pulsed Power," Digest of Technical Papers: Tenth IEEE Pulsed Power Conference (IEEE, Piscattaway NJ, 1996).

27. Lindemuth, I.R., et al., "Joint US/Ryssian Plasma Formation Experiments for Magnetized Target Fusion (MTF)," Digest of Technical Papers: Tenth IEEE Pulsed Power Conference (IEEE, Piscattaway NJ, 1996).

28. Siemon, R.E., et al., "Magnetized Target Fusion: Principles and Status," IAEA Technical Committee Meeting on Innovative Approaches to Fusion (Pleasanton, CA, October 1997).

29. Siemon, R.E., et al., "Magnetized Target Fusion," invited paper at DOE Office of Fusion Energy Sciences Innovative Confinement Concepts Workshop (Los Angeles, CA, March_3-8, 1997)

30. Sheehey, P.T., et al., "Integrated Computational Modeling of Liner-On-Plasma Fusion Experiments," Proceedings of Ninth Nuclear Explosives Code Developers Conference (NECDC) (SanDiego, CA, October 1996); and Am. Phys. Soc. Plasma Physics Division (Denver, CO, October 1996).

31. Younger, S.M., et al., "Lab-to-Lab Scientific Collaborations Between Los Alamos and Arzamas-16 Using Explosive-Driven Compression Generators," Los Alamos Science **24**, 48 (1996).

32. Hecker, S., et al., "Side by Side as Equals -- An Unprecidented Collaboration between Russian and American Nuclear Weapons Laboratories to Reduce the Nuclear Danger," Los Alamos Science **24**, 48 (1996).

References

[1] Lindl, J.D., "Physics of Ignition for ICF Capsules," Inertial Confinement Fusion Course and Workshop (Varenna, Italy, 1988, A. Caruso and E. Sindoni, ed.)

[2] Gerwin, R.A., and Malone, R.C., "Adiabatic Plasma Heating and Fusion Energy Production by a Compressible Fast Liner," Nuclear Fusion 19, 155 (1979).

[3] Kirkpatrick, R. C., Lindemuth, I. R. and Ward, M. S., "An Overview of Magnetized Target Fusion," Fusion Technology 27, p. 201 (1995).

[4] R.C. Kirkpatrick and D.P. Smitherman, "Energetic Alpha Transport in a Magnetized Fusion Target", Proceedings of the 12th Topical Meeting on the Technology of Fusion Energy (1996 American Nuclear Society Annual Meeting) Reno, NV, June 1996.

[5] Widner, M.M., "Neutron Production from Relativistic Electron Beam Targets," Bull. Am. Phys. Soc. 22, 1139 (1977).

[6] Lindemuth, I.R., and M.M. Widner, M.M., "Magnetohydrodynamic Behavior of Thermonuclear Fuel in a Preconditioned Electron Beam Imploded Target," Phys. Fluids 24, 753 (1981).

[7] Lindemuth, I.R., and Kirkpatrick, R. C., "Parameter Space for Magnetized Fuel Targets in Inertial Confinement Fusion," Nuclear Fusion 23, 263 (1983).

[8] Buyko, A.M., Chernyshev, V.K., Demidov, V.A., et al., "Investigations of Thermonuclear Magnetized Plasma Generation in the Magnetic Implosion System MAGO," in Physics of High Energy Densities, MEGAGAUSS VI, Albuquerque, NM (1992).

[9] Idzorek, G. C. and Oona, H., "Soft x-ray diagnostics for MAGO Experiments," DOE Innovative Confinement Concepts Workshop (Marina del Rey, March 1997).

[10] Kirkpatrick, R.C., "Shock Analysis for the MAGO III experiment," Los Alamos internal memo NIS-9(U)-96-115 (1996); "Diagnostic Hole Shocks in the MAGO Experiments," Los Alamos internal memo NIS-9(U)-96-122 (1996).

[11] Foster Evans, "Note on the Calculation of Energy Deposition of Alpha Particles in a DT Plasma by Rutherford Scattering," LA-5448-MS, Los Alamos National Laboratory (1973).

[12] R. Cooper and F. Evans, Phys. Fluids, 18, 332 (1975).

[13] M. J. Antal and C. E. Lee, "Charged particle energy deposition in an inertially confined thermonuclear plasma," Nucl. Science & Engineering, 64, 379-383 (1977).

[14] E. G. Corman, W. E. Lowe, G. Cooper and A. Winslow, Nucl. Fusion, 15, 377 (1975).

[15] S. Atzeni, Plasma Phys. Control. Fusion, 29, p. 1535 (1987).

[16] M. M. Basko, Nucl. Fusion, 30, p. 2443 (1990).

[17] A. M. Oparin, S. I. Anisimov, J. Meyer-Ter-Vehn, "Kinetic simulation of DT Ignition and burn in ICF targets," Nucl. Fusion, 36, p. 443 (1996).

[18] S. Wang and L. Qiu, "Alpha Particle Classical Transport in Tokomaks," Nuclear Fusion 36 (1996) 557.

[19] S.J. Zweben, et al., "Alpha Particle Loss in the TFTR DT Experiments," Nuclear Fusion 35 (1995) 893.

[20] M.H. Redi, et al., "Collisional Stochastic Ripple Diffusion of Alpha Particles and Beam Ions on TFTR," Nuclear Fusion 36 (1996) 1193.

[21] Schoenberg, K.F., Gerwin, R. A., Moses, R.W. Jr., and Sheehey , P. T., "Near-term Prospects for Magnetized Target Fusion Using the ATLAS Experiment," DOE Innovative Confinement Concepts Workshop (Marina del Rey, March 1997).

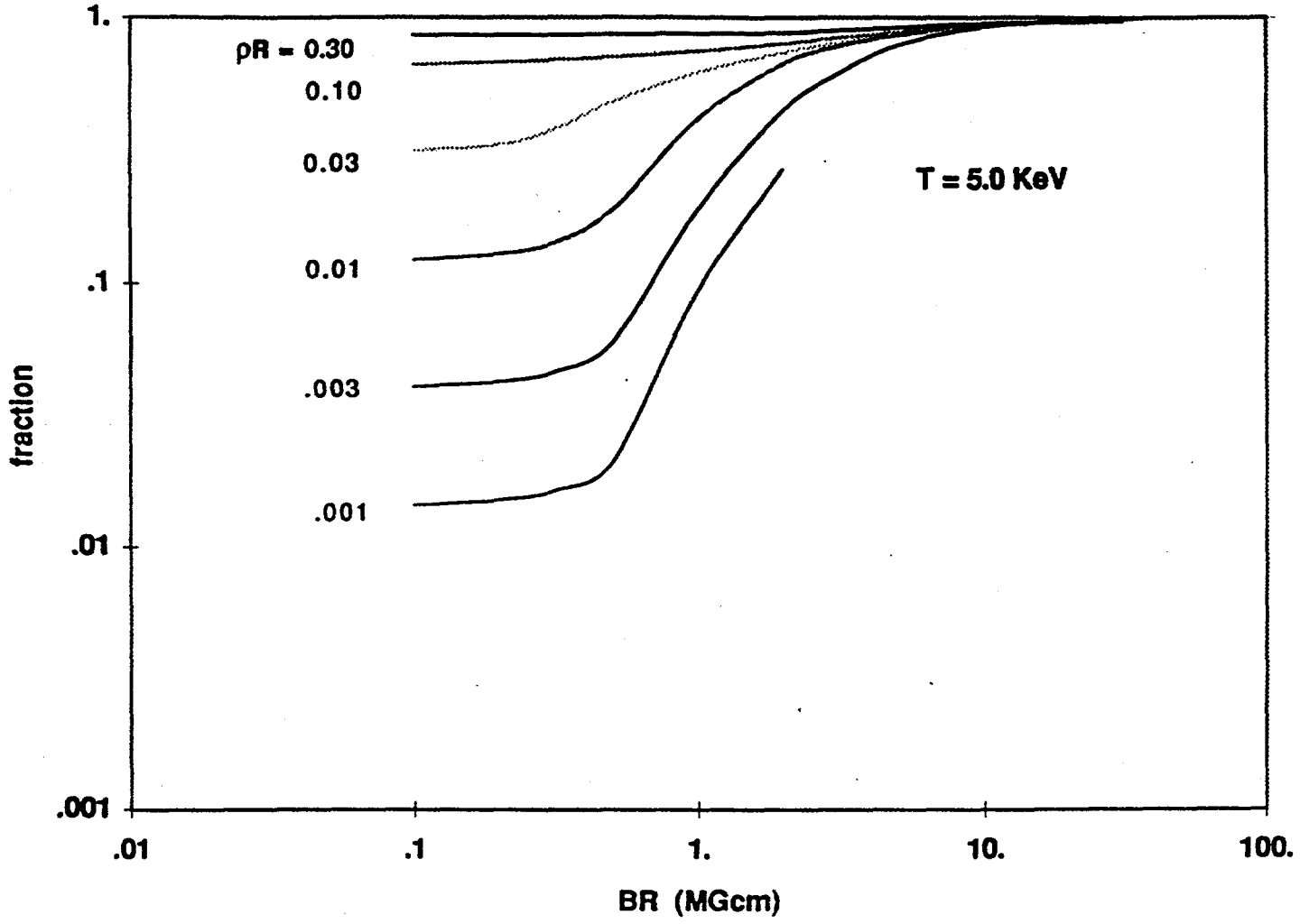

Figure 1: DT fusion alpha particle fractional energy deposition in a uniform spherical plasma at 5 KeV.

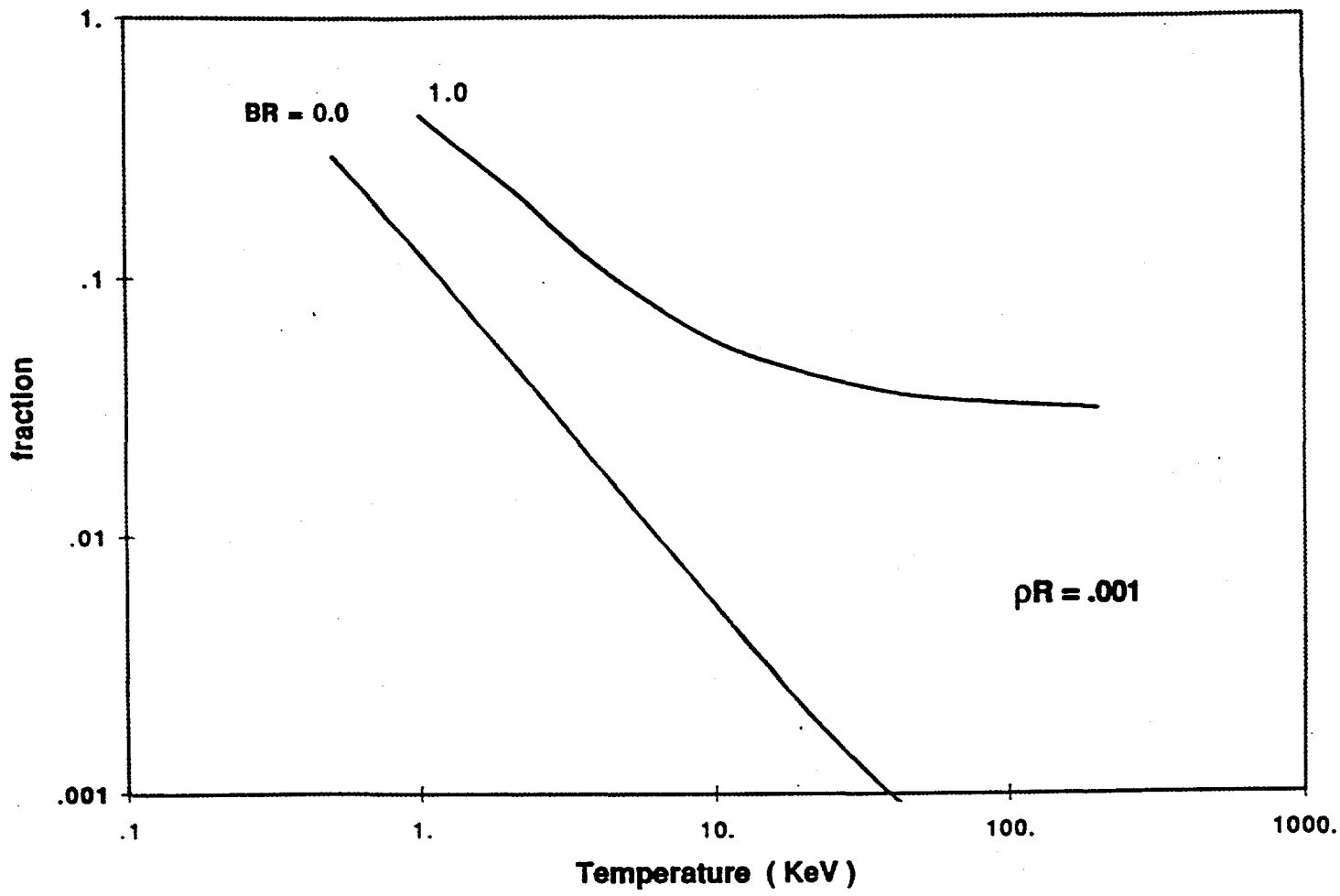

Figure 2: DT alpha fractional energy deposition with and without a magnetic field.

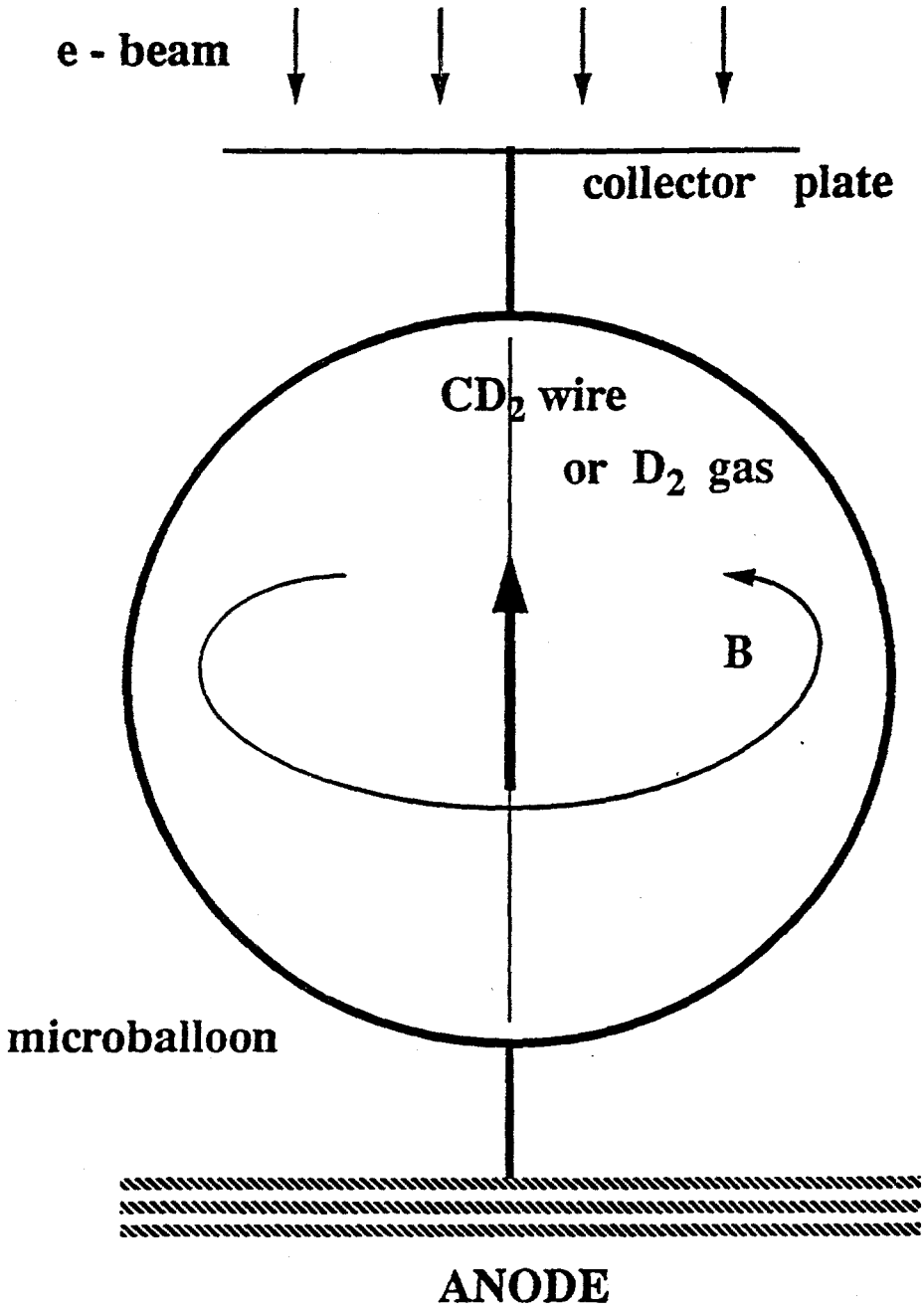

Figure 3: Sandia Phi-target

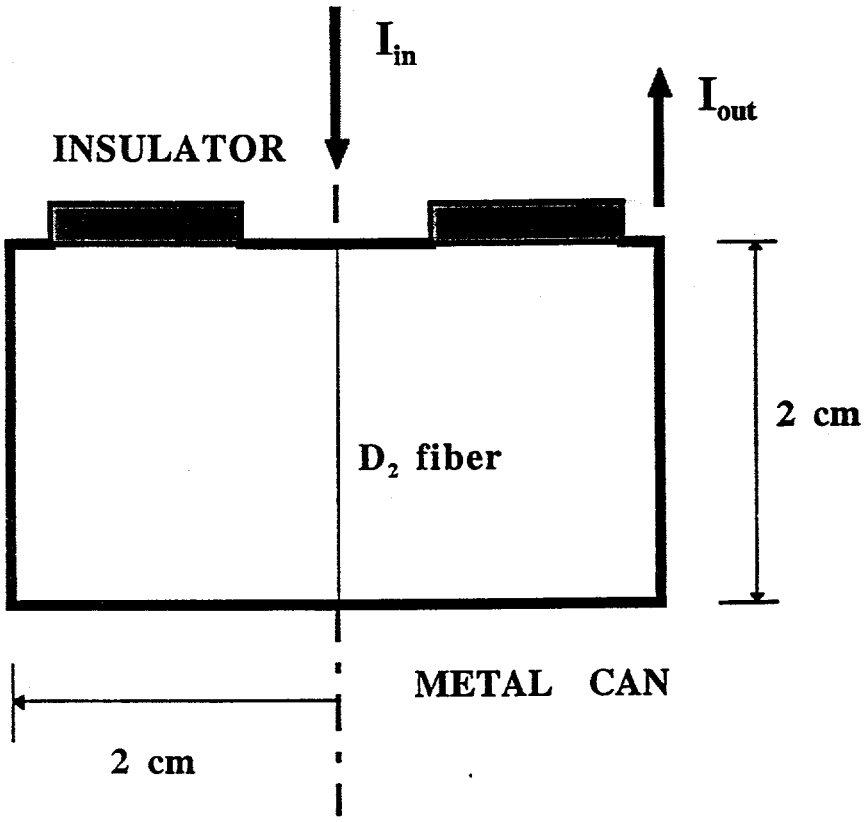

Figure 4: Cyrogenic fiber in a can, the Colt target plasma generation experiment.

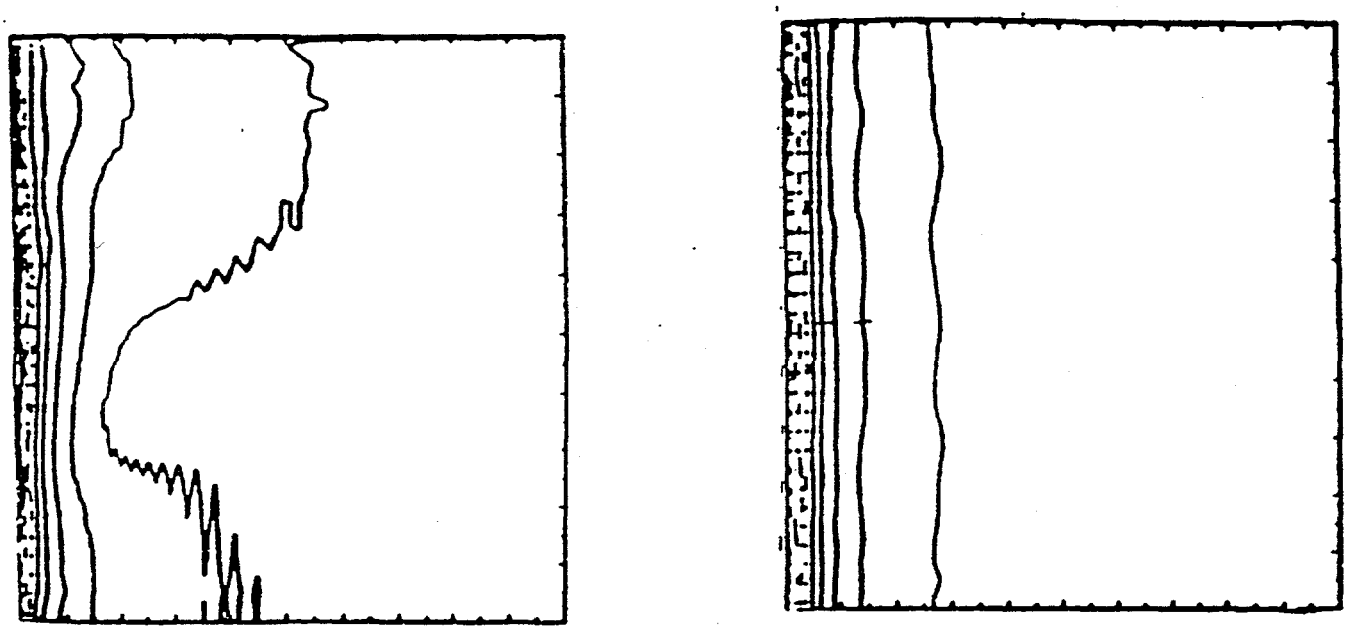

Figure 5: Calculated axial current contours (r-z 2 cm by 2 cm). Stablization of the Z-pinch occurs as wall support comes into play: The left contours are for 1.1 μs and the right for 2.4 μs.

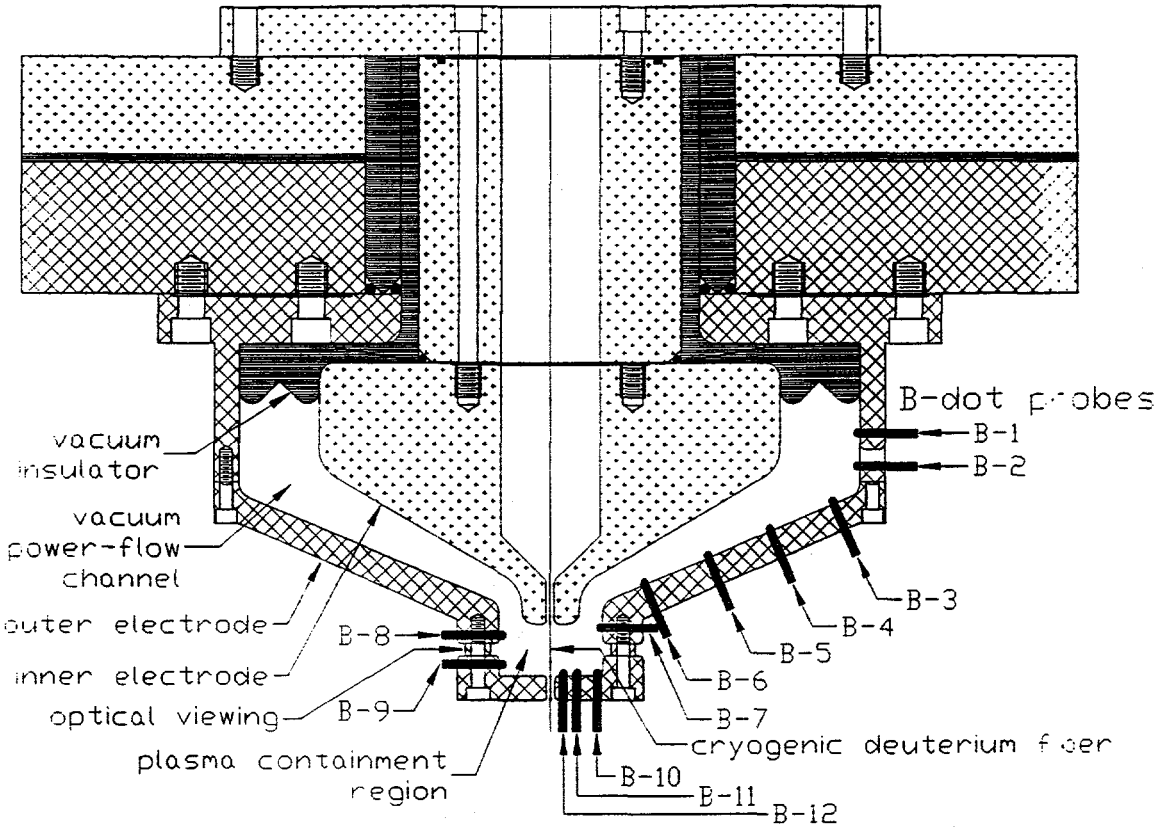

Figure 6: Experiment as implemented on Colt.

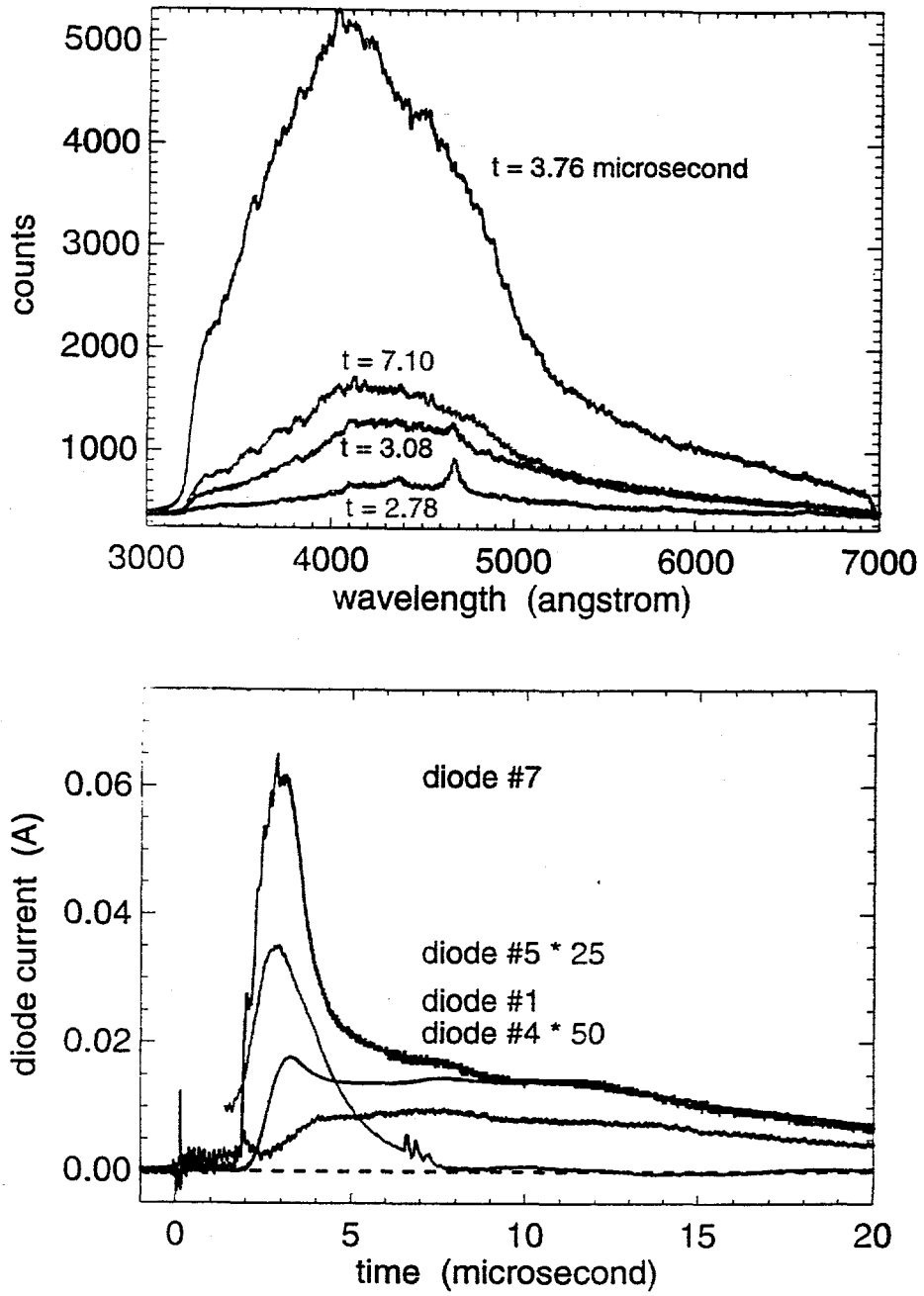

Figure 7: The upper graph shows optical spectroscopic data from discharges with an erected bank voltage of 40 KV. The data in the upper graph are from a gated OMA visible spectrometer with a 330 ns gate-width. The times are, in order of decreasing signal magnitude, 3.76 μs, 7.10μs, 3.08μs, and 2.78μs. These discharges had 1torr of hydrogen fill. The data in the lower graph are unfiltered and filtered photodiode data for a discharge with 1.36 torr of hydrogen and an erected bank voltage of 66 kV. In order of decreasing peak signal magnitude (as plotted with the stated multipliers) is diode #7, #5 (multiplied by 25), #1, and #4 (multiplied by 50). There is good shot-to-shot reproducibility for the diode signals except for diode #5, which has varied from zero signal to over twice that shown in this plot for discharges where all other diagnostics show little shot-to-shot differences.

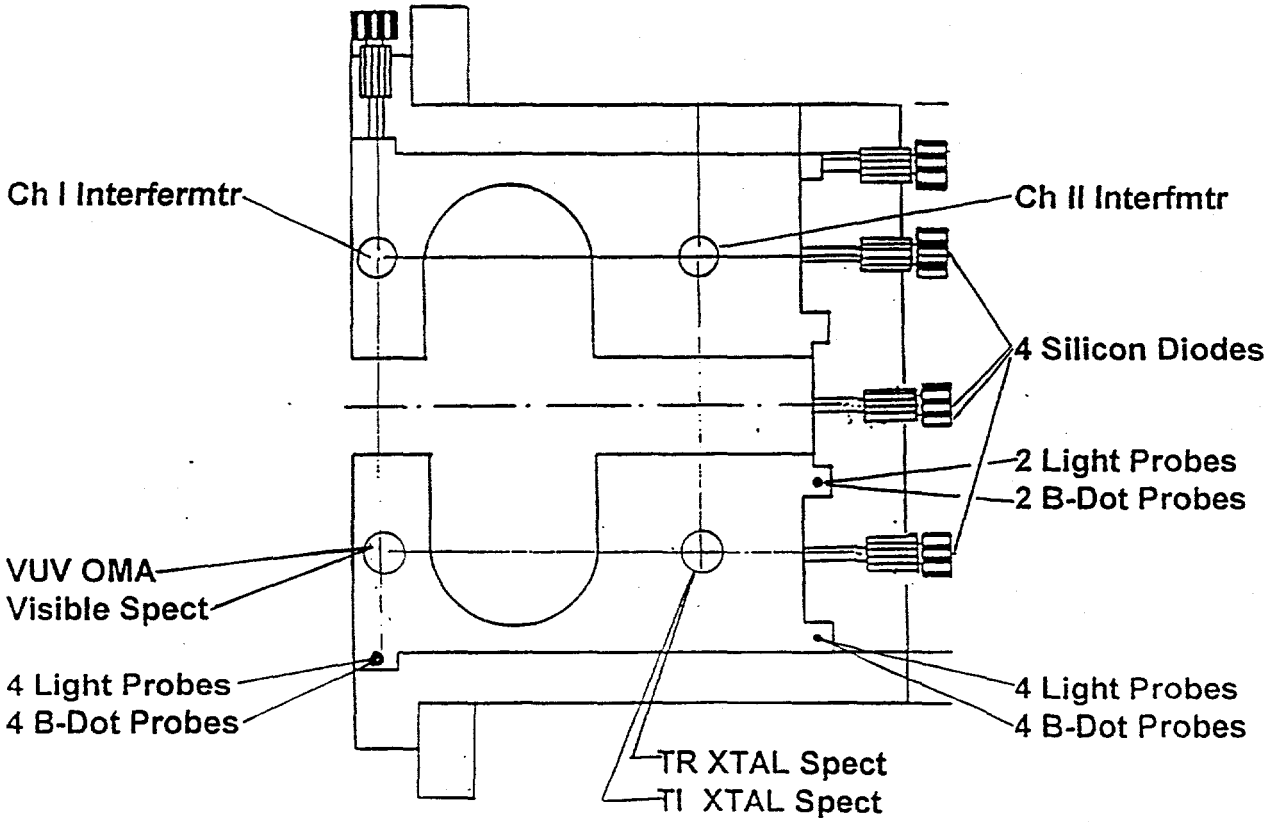

Figure 8: MAGO II configuration and diagnostic access.

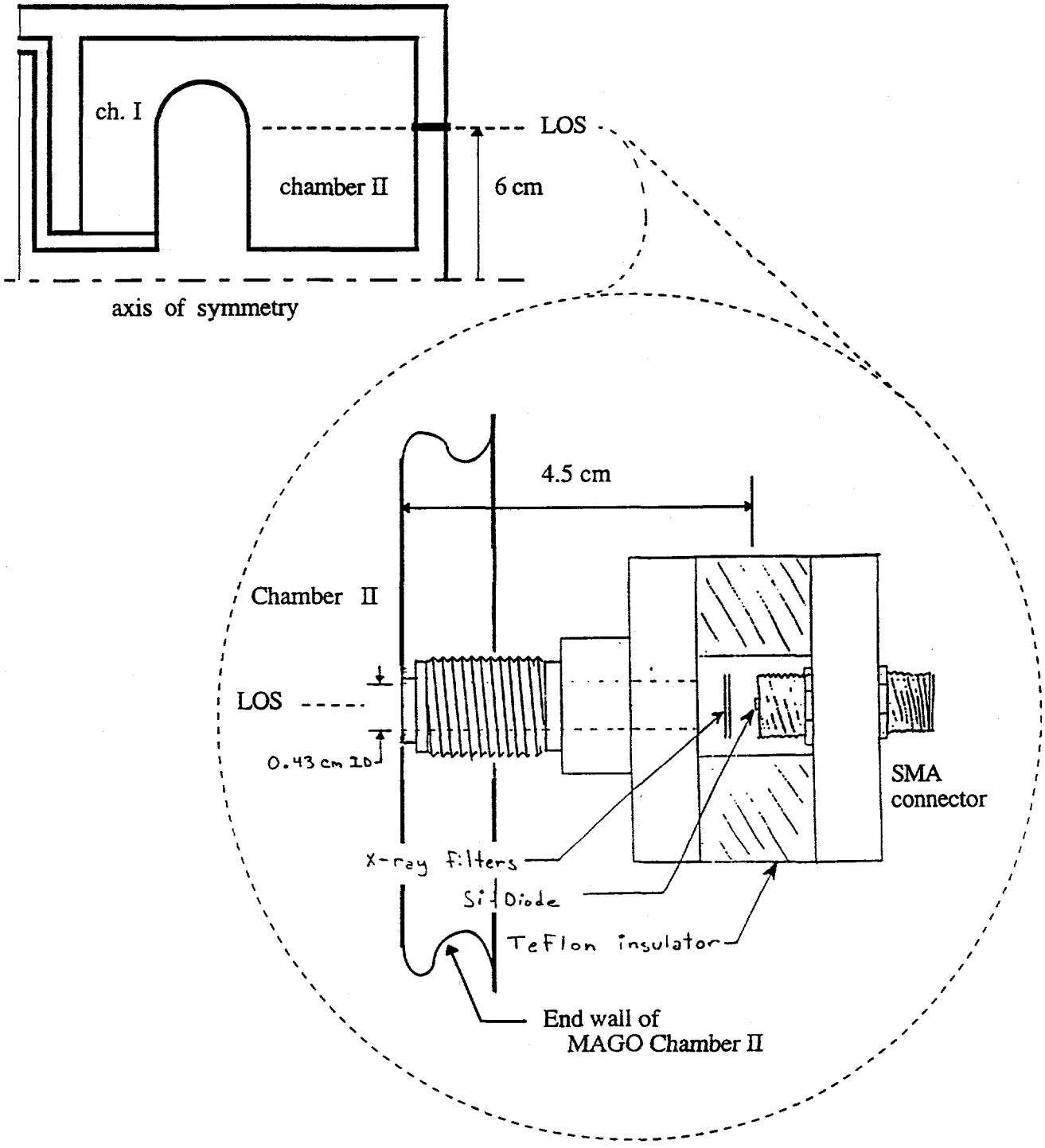

Figure 9: Mounting of a filtered diode in an assembly for mounting on the chamber wall.

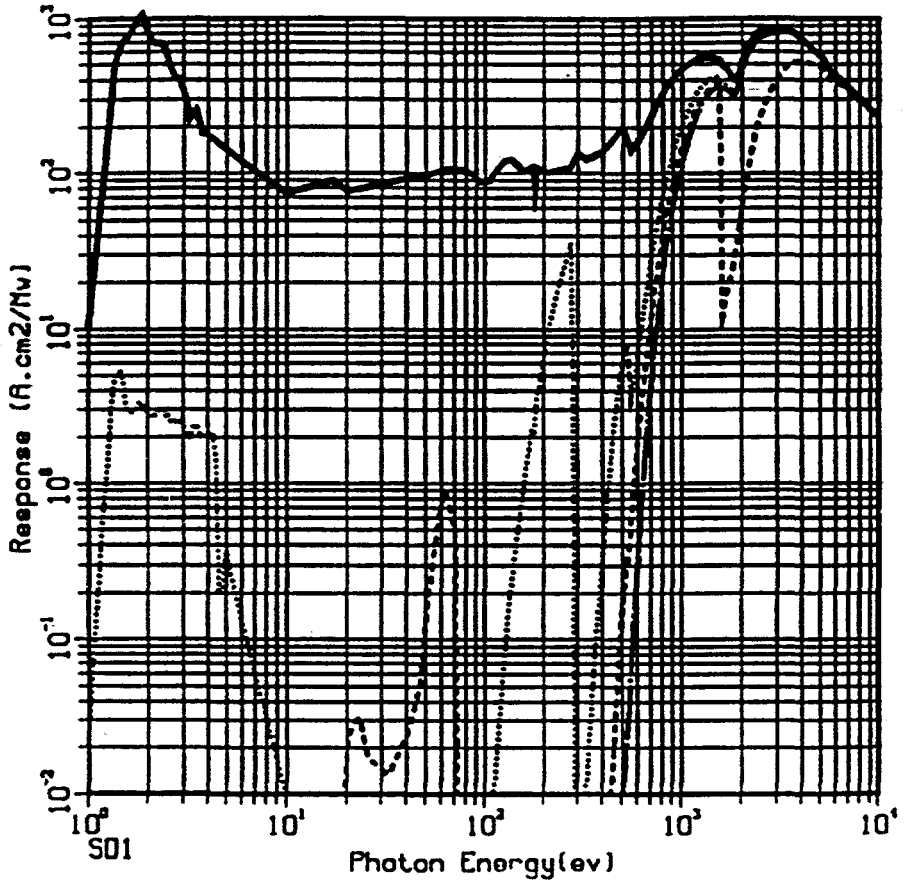

Figure 10. Filtered silicon diode response curves.

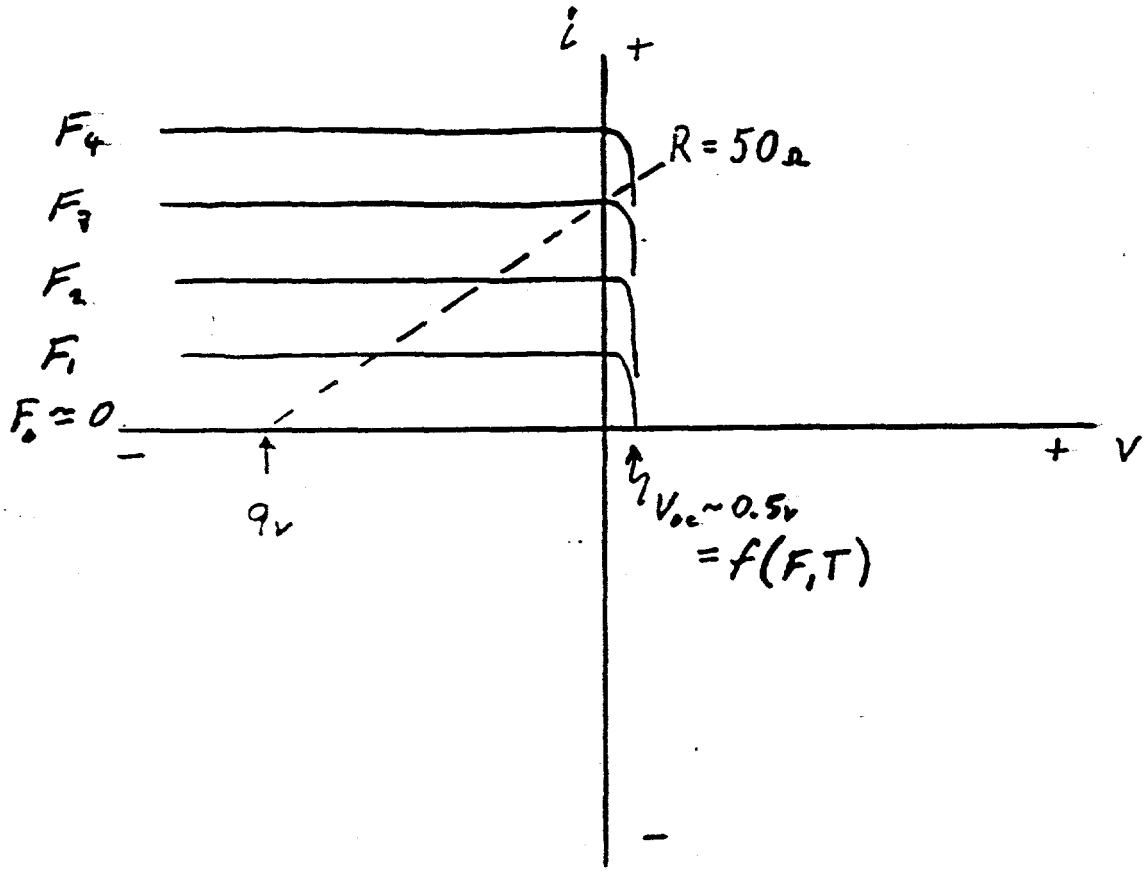

Figure11: Typical silicon photodiode diode characteristic curves.

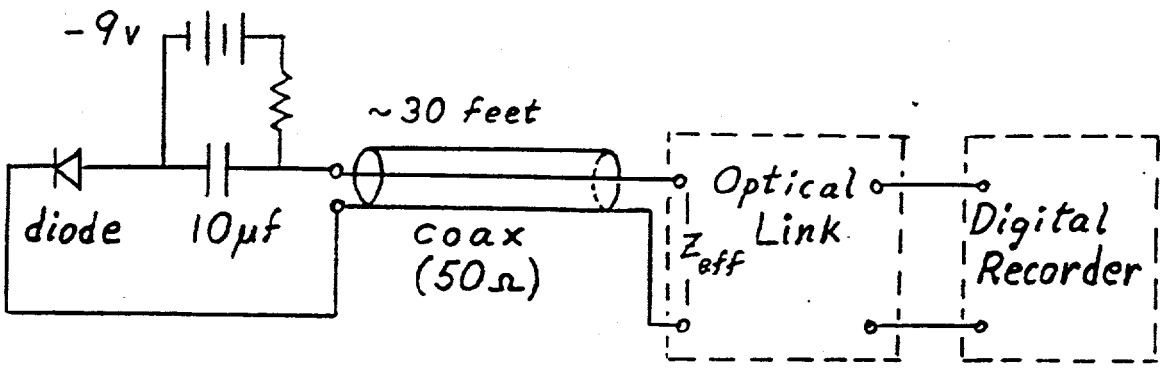

Figure 12: Detector circuit.

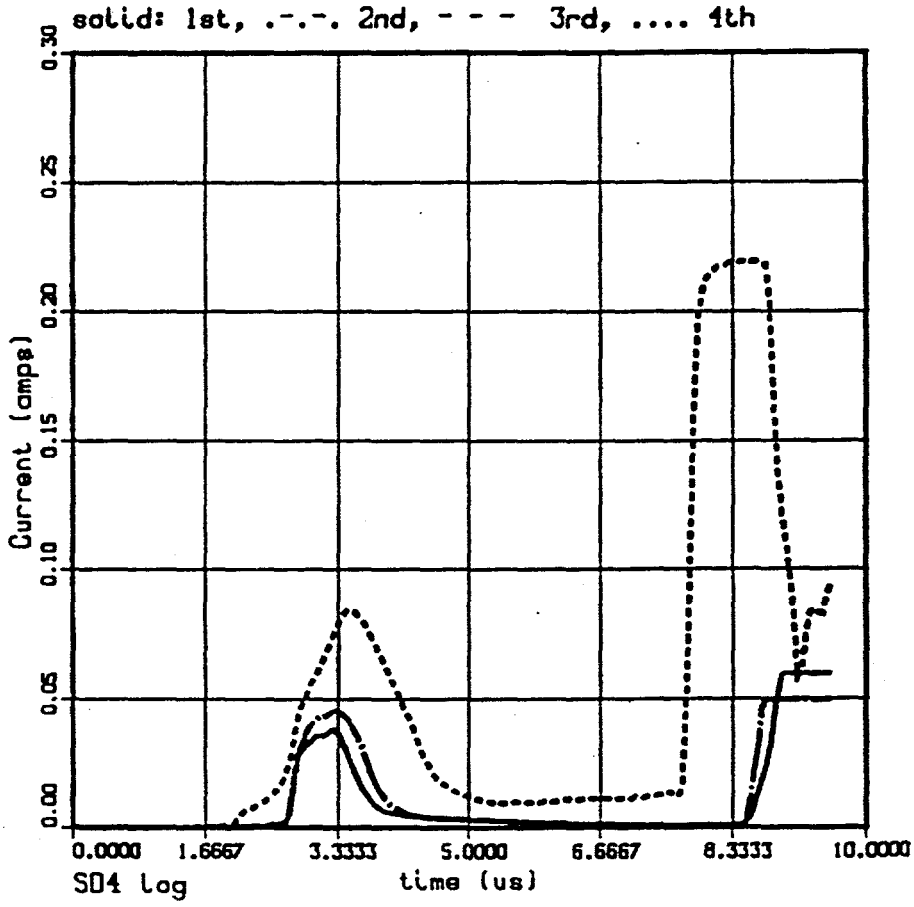

Figure 13: Data for the three MAGO II filtered silicon diodes looking along the 6 cm line of sight. Zero on the time axis corresponds to 347.0 μs in the MAGO III data files.

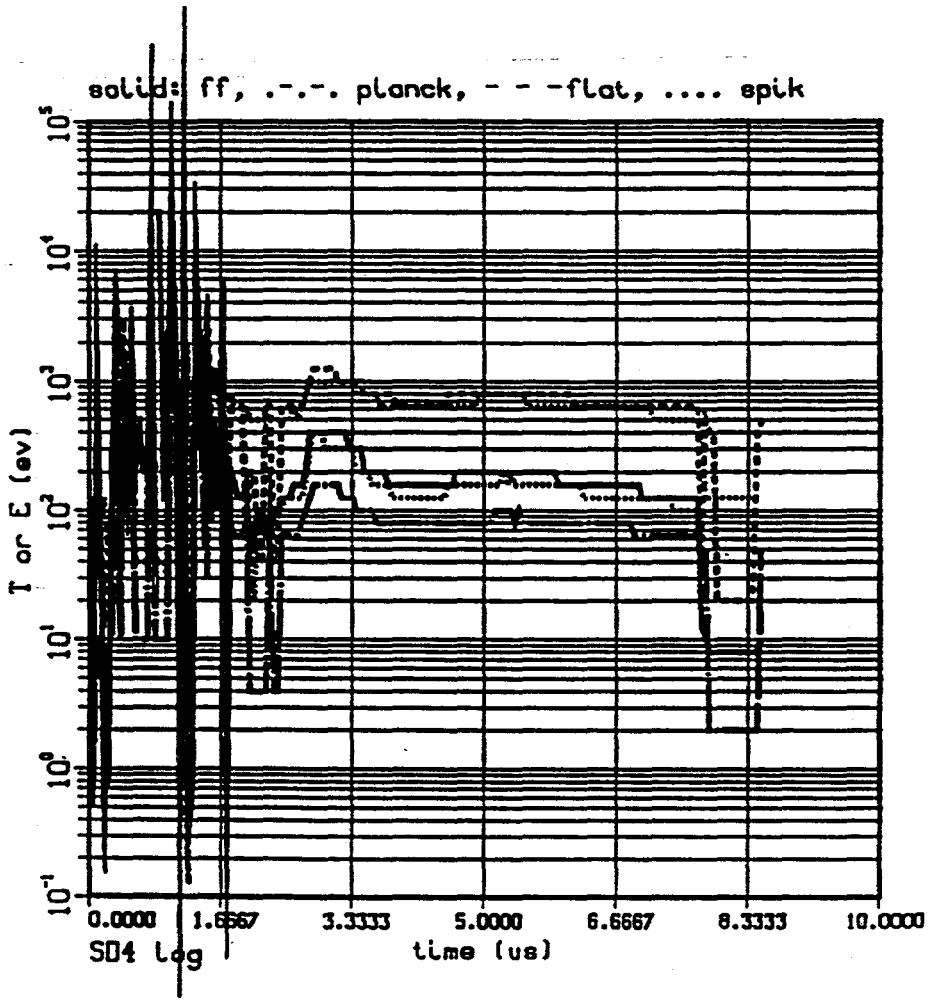

Figure 14. Inferred temperature or characteristic energy history for 5 spectral types: Planck, bremsstrahlung, flat spectrum, single energy, and exponential spectrum.

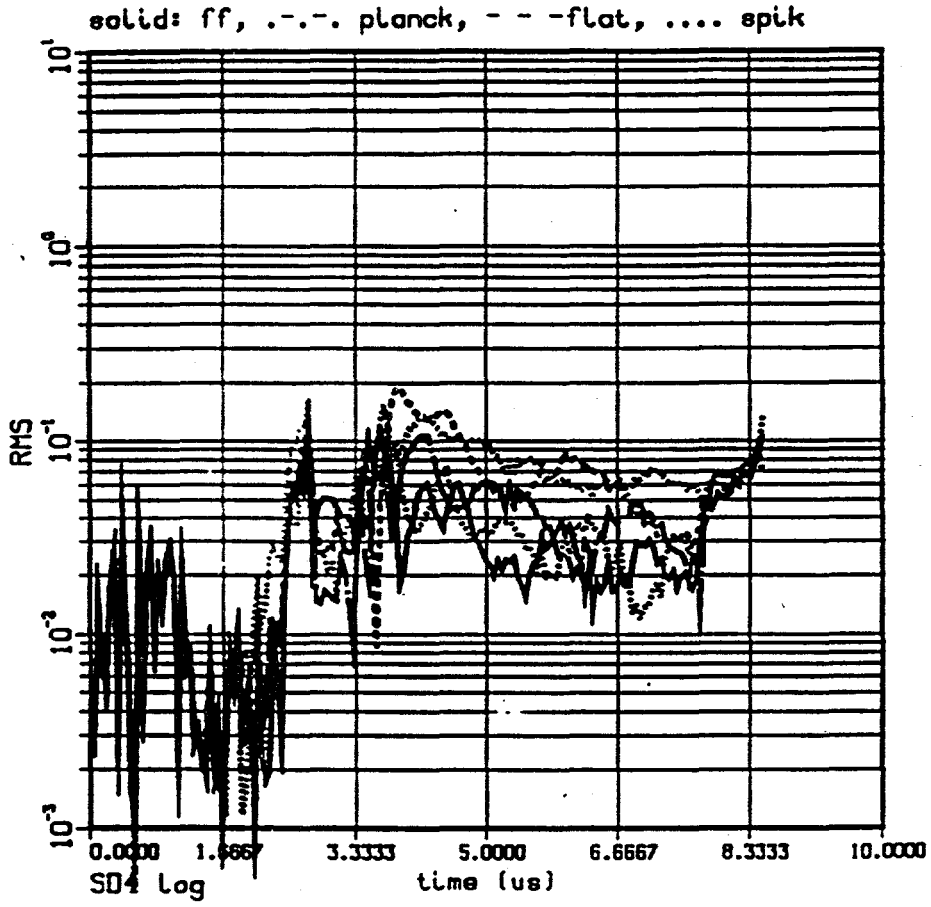

Figure 15. Fractional root-mean-square best fit of assumed spectrum to data. During the time when the signal to noise ratio (S/N) is high, the bremsstrahlung spectrum generally gives the best rms fit to the data, but other spectral types sometimes are better.

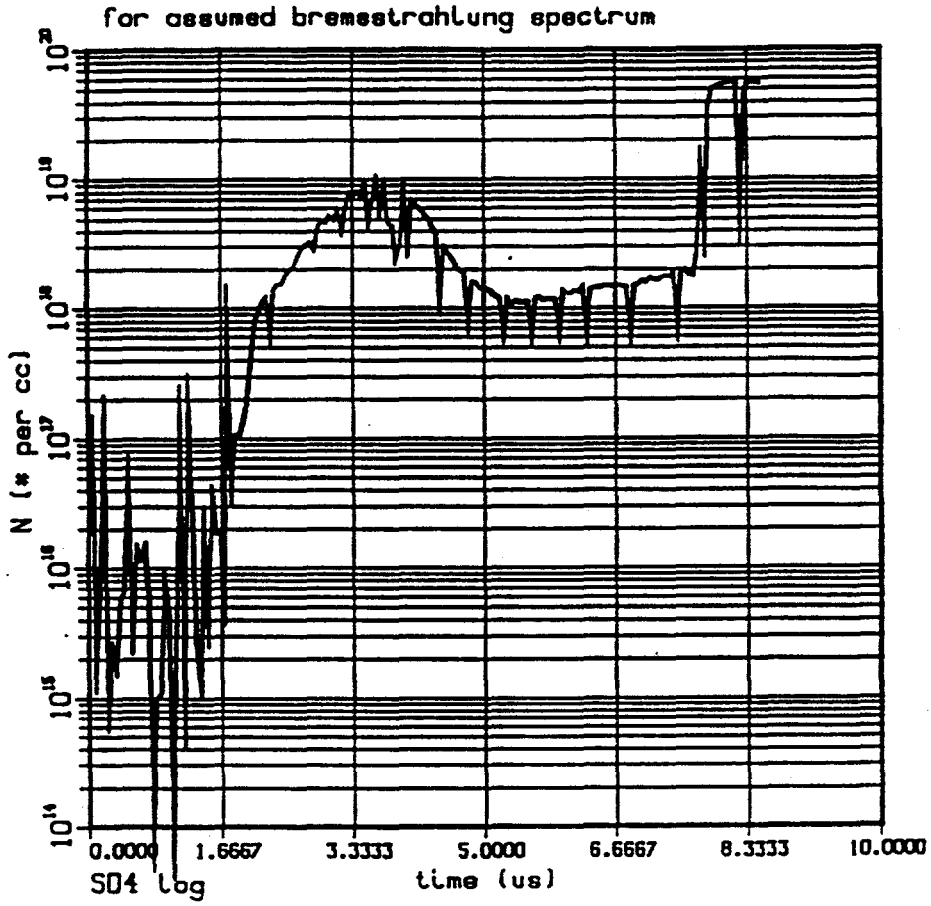

Figure 16. Estimated density for a bremstrahlung spectrum, assuming that the emission depends on the square of the density.

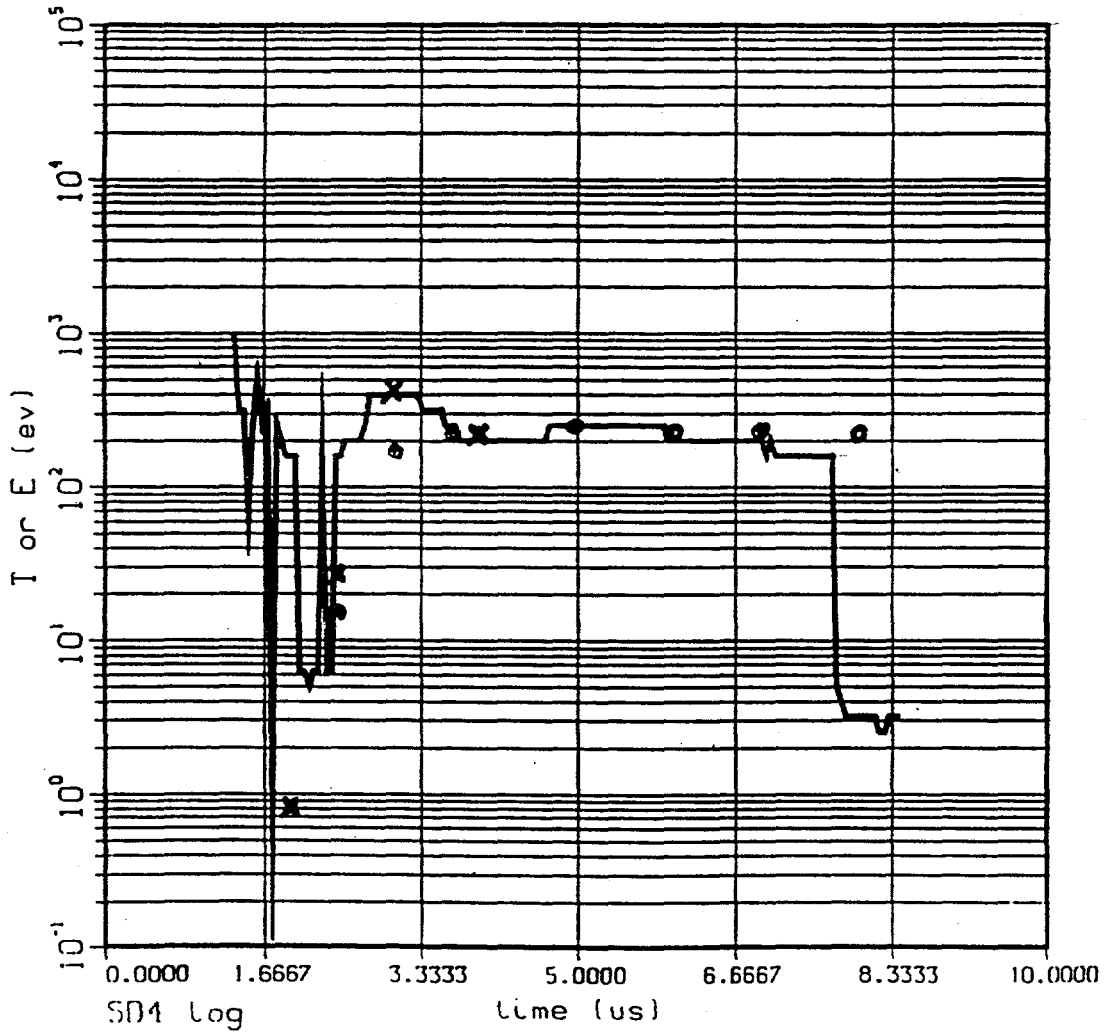

Figure 17. MAGO II temperature history with the 0.01 % neon included using spectra synthesized by ZAP. The points (x's and o's for 1-T and 2-T) are the averages along the diagnostic line of sight as computed by the 2-D MHD code.

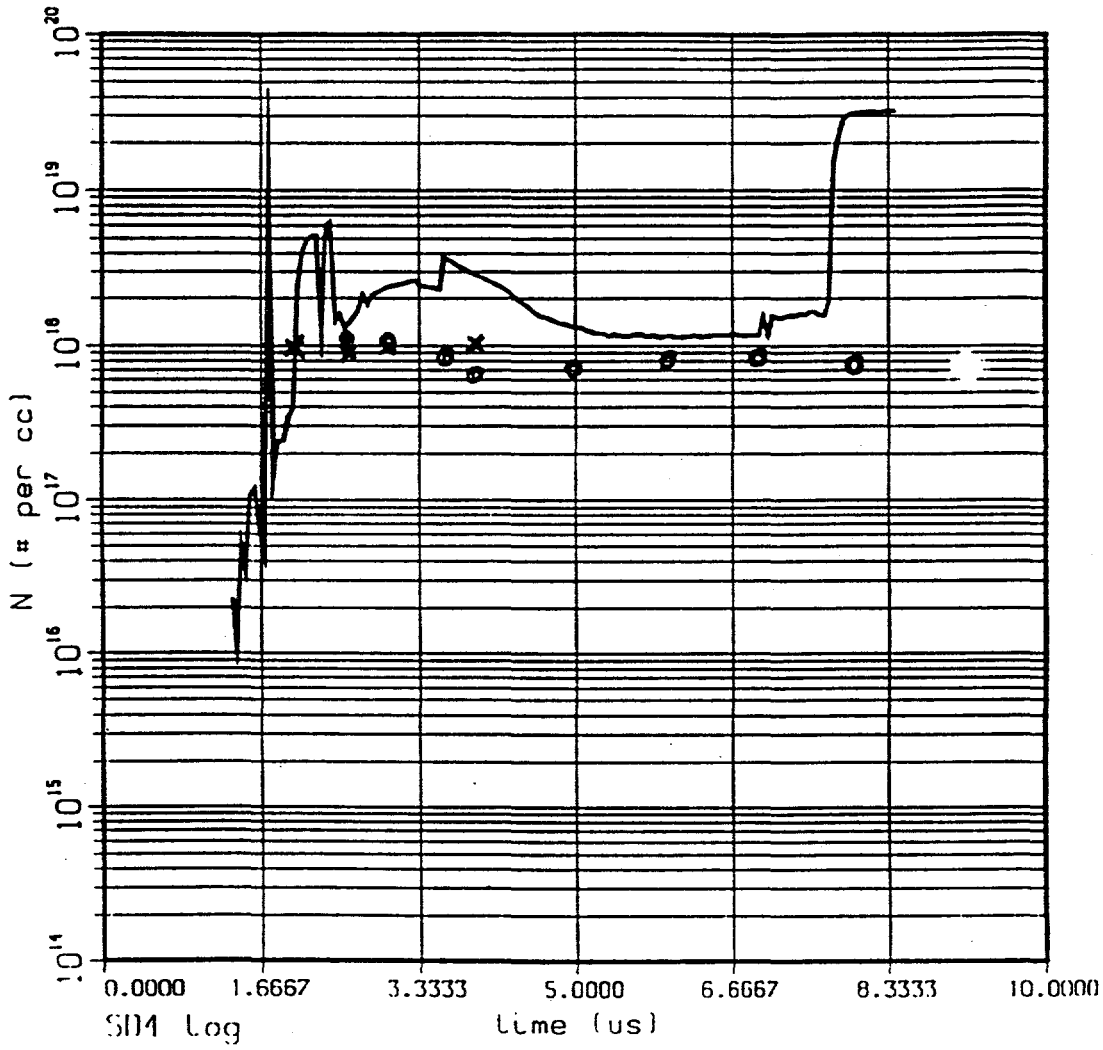

Figure 18: The commensurate estimated density history derived for the synthesized spectra is shown. The points (x's and o's for 1-T and 2-T) are the averages along the diagnostic line of sight as computed by the 2-D MHD code.

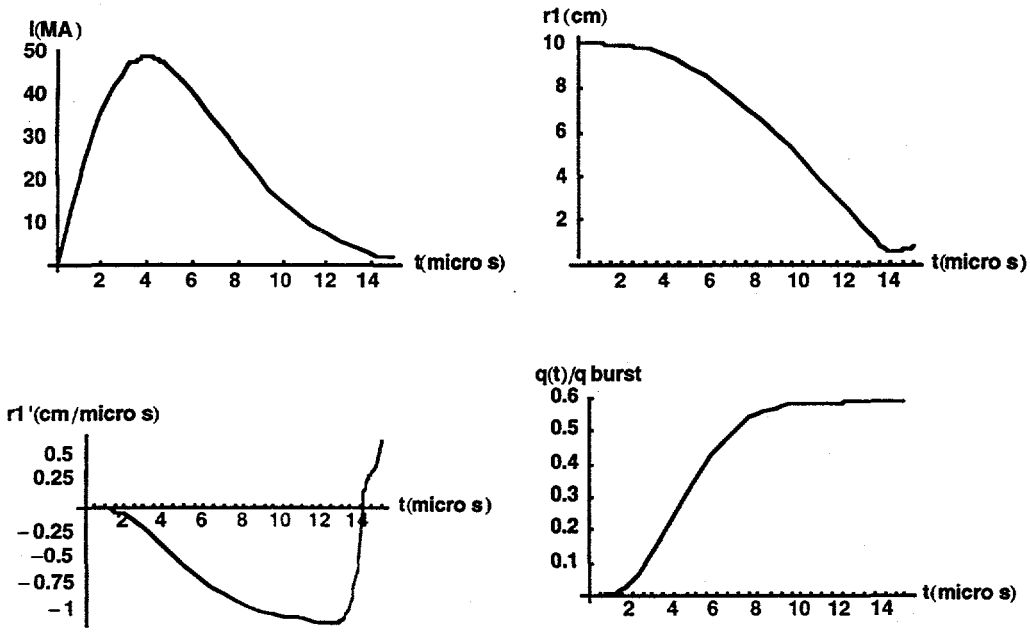

Figure 19. Liner current, I; plasma radius, r_1; plasma edge velocity, r_1'; and liner ohmic heating compared to the burst condition as functions of time for compression of an ideal plasma in aforementioned Atlas conditions.

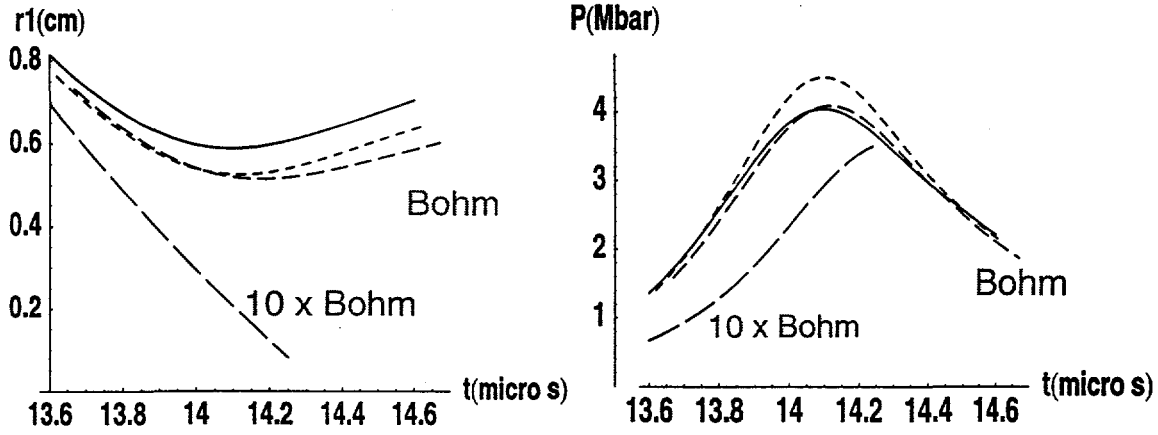

Figure 20. Plasma radius and pressure as functions of time for adiabatic plasma, solid curves; classical plasma with bremsstrahlung radiation, short dashes; Bohm thermal conduction and bremsstrahlung, intermediate dashing; and 10× Bohm thermal conduction plus bremsstrahlung, long dashes.

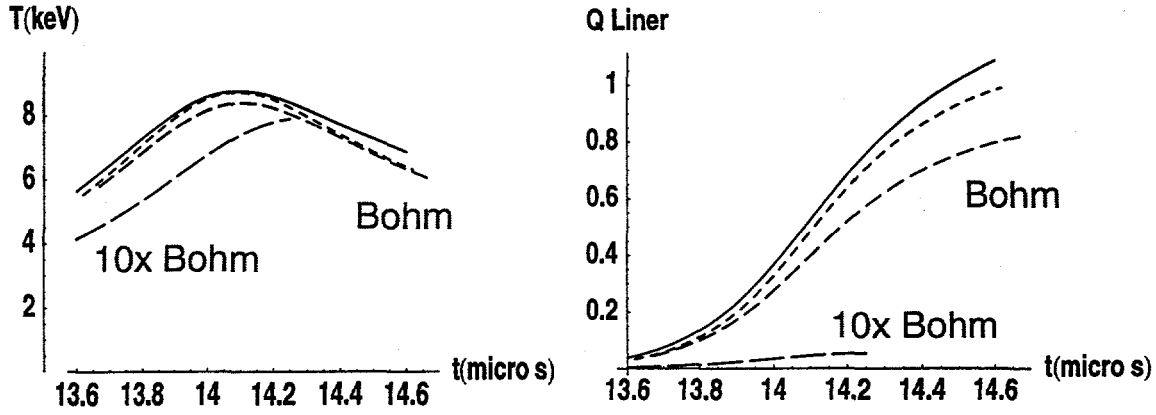

Figure 21. Plasma temperature and liner Q fusion yield/peak liner kinetic energy) as functions of time for adiabatic plasma, solid curves; classical plasma with bremsstrahlung radiation, short dashes; Bohm thermal conduction and bremsstrahlung, intermediate dashing; and 10× Bohm thermal conduction plus bremsstrahlung, long dashes.

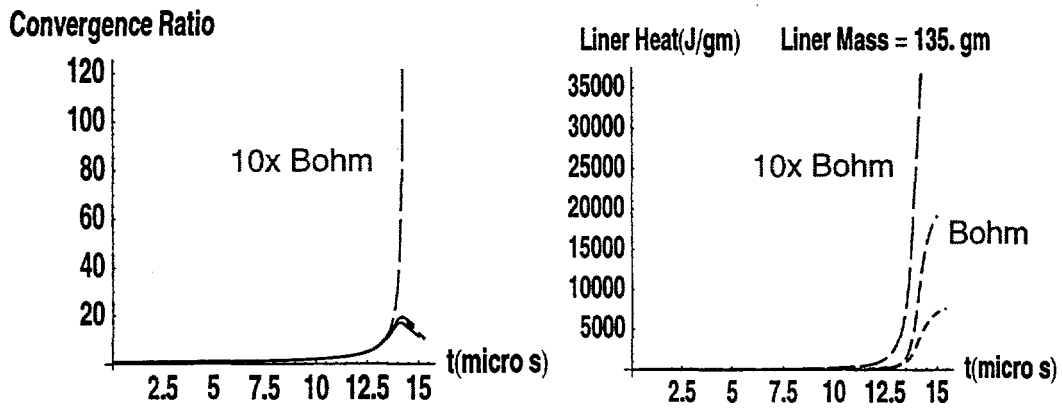

Figure 22. Liner convergence and heat load to the liner as functions of time for adiabatic plasma, solid curves; classical plasma with bremsstrahlung radiation, short dashes; Bohm thermal conduction and bremsstrahlung, intermediate dashing; and 10× Bohm thermal conduction plus bremsstrahlung, long dashes.